Cell Systems

Article

Human macrophages encode stimulus-specific information of prior exposures through trained immunity

Graphical abstract

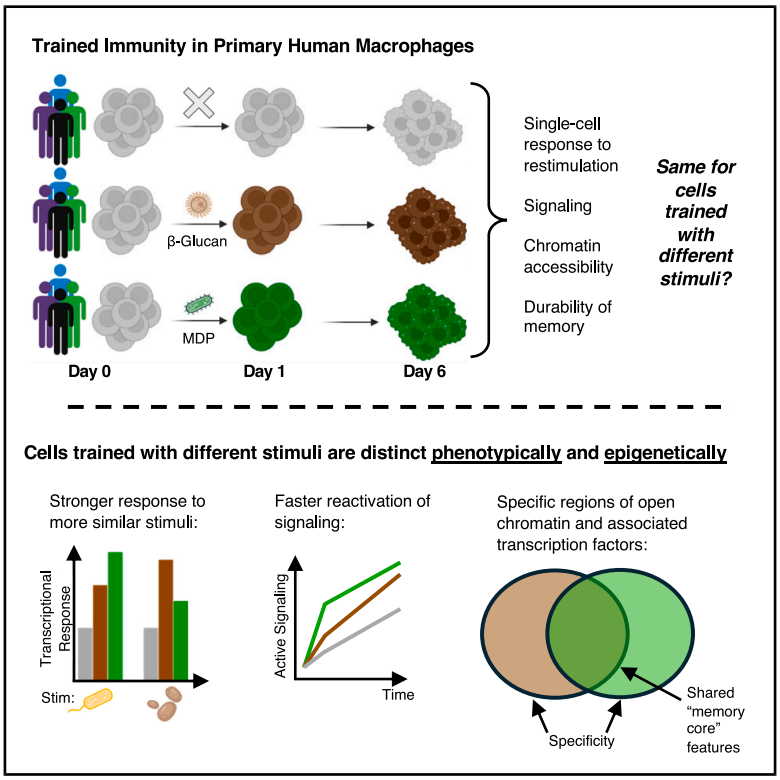

Highlights

- Trained immunity in human macrophages is stimulus specific
- Trained cells respond more strongly to stimuli similar to the inducing stimulus
- Epigenetics of trained cells have both stimulus-specific and shared features
- Durability of epigenetic and phenotypic trained states is stimulus specific

Authors

Aoife O'Farrell, Zijian Niu, Jingxin Li, Laura C. Van Eyndhoven, Kavitha Sarma, Arjun Raj

Correspondence

arjunrajlab@gmail.com

In brief

Innate immune cells can remember prior experiences with pathogens. Here, O'Farrell et al. provide quantitative measurements of stimulus specificity of trained innate immune memory in primary human monocyte-derived macrophages. Specificity in the trained state exists within epigenetic, transcriptomic, proteomic, and signaling compartments of a trained macrophage.

O'Farrell et al., 2026, Cell Systems *17*, 101647
July 15, 2026
https://doi.org/10.1016/j.cels.2026.101647

CellPress

Cell Systems

CellPress

Article

Human macrophages encode stimulus-specific information of prior exposures through trained immunity

Aoife O'Farrell,[1] Zijian Niu,[2,3,4] Jingxin Li,[5] Laura C. Van Eyndhoven,[1] Kavitha Sarma,[6,7] and Arjun Raj[1,8,9,*]
[1]Department of Bioengineering, School of Engineering and Applied Sciences, University of Pennsylvania, Philadelphia, PA, USA
[2]Department of Chemistry, School of Arts and Sciences, University of Pennsylvania, Philadelphia, PA, USA
[3]Department of Physics and Astronomy, School of Arts and Sciences, University of Pennsylvania, Philadelphia, PA, USA
[4]Computational and Systems Biology Program, Massachusetts Institute of Technology, Cambridge, MA, USA
[5]Genetics and Epigenetics, Cell and Molecular Biology Graduate Group, Perelman School of Medicine, University of Pennsylvania, Philadelphia, PA, USA
[6]The Wistar Institute, Gene Expression and Regulation Program, Philadelphia, PA, USA
[7]Department of Cell and Developmental Biology, Perelman School of Medicine, University of Pennsylvania, Philadelphia, PA, USA
[8]Department of Genetics, Perelman School of Medicine, University of Pennsylvania, Philadelphia, PA, USA
[9]Lead contact
*Correspondence: arjunrajlab@gmail.com
https://doi.org/10.1016/j.cels.2026.101647

SUMMARY

Trained immunity (a form of innate immune memory) is defined in part by heightened responses to pathogen restimulation and can be generated by many different stimuli. However, both the quantitative differences in trained states generated by different stimuli and the downstream consequences of those differences remain unclear. Here, we used primary human monocyte-derived macrophages to demonstrate phenotypic and molecular stimulus specificity of trained immunity 6 days after initial exposure. Quantification of cytokine production with single-molecule RNA imaging revealed stimulus-specific patterns of response to restimulation, with trained cells showing stronger responses to secondary stimuli more similar to their initial stimulation. Differential licensing of inflammatory transcription factors was associated with encoding of specificities in chromatin 6 days after training, while memory of some, but not all, training stimuli was lost by 11 days post-training *in vitro*. Overall, our findings demonstrate that different training stimuli can impart specific memories that generate distinct training phenotypes.

INTRODUCTION

Although once believed incapable of forming memory, macrophages are now understood to change functionally following an encounter with an inflammatory stimulus. One such form of innate immune memory is trained immunity, or training, through which macrophages return to a resting inflammatory baseline but mount a stronger and faster inflammatory response to restimulation.[1–3] Training is typically contrasted with priming memory, whereby cells retain elements of immune activation following initial stimulation (such as active immune gene transcription), and "tolerance" memory, whereby cells mount a weaker response to restimulation.[3]

By these definitions, many different stimuli are capable of generating trained immunity, including pathogen-associated molecular pattern (PAMP) stimulation *in vitro*,[4–6] vaccination,[7–9] infection *in vivo*,[10,11] host factors,[12,13] and tissue injury.[14,15]

Most studies of trained immunity emphasize qualitative effects of training that are *shared* across these distinct training stimuli, including functional protection from infection,[9,16,17] metabolic changes,[18,19] or increased production of key cytokines such as *TNF* and *IL6*.[7,12] Comparatively less focus, however, has been placed on possible differences in the trained states that are induced by different training stimuli. Efforts to compare trained states *post facto* typically rely on meta-analyses of published literature.[3,20] However, observed phenotypes of trained immunity are incredibly sensitive to even subtle differences in experimental design[21,22] and to genetic and non-genetic differences across individual human donors,[23,24] motivating the need for direct comparison of trained states in a highly controlled, quantitative manner.

Recent experimental efforts to make these direct comparisons have indeed revealed longer-term (1–4 weeks after stimulation) epigenetic[25,26] and transcriptomic[26,27] differences in trained states generated by different stimuli, adding to earlier work demonstrating specificity of innate immune memory at short timescales (around 24 h after stimulation).[28–31] Other forms of innate immune memory, including the formation of

Please cite this article in press as: O'Farrell et al., Human macrophages encode stimulus-specific information of prior exposures through trained immunity, Cell Systems (2026), https://doi.org/10.1016/j.cels.2026.101647

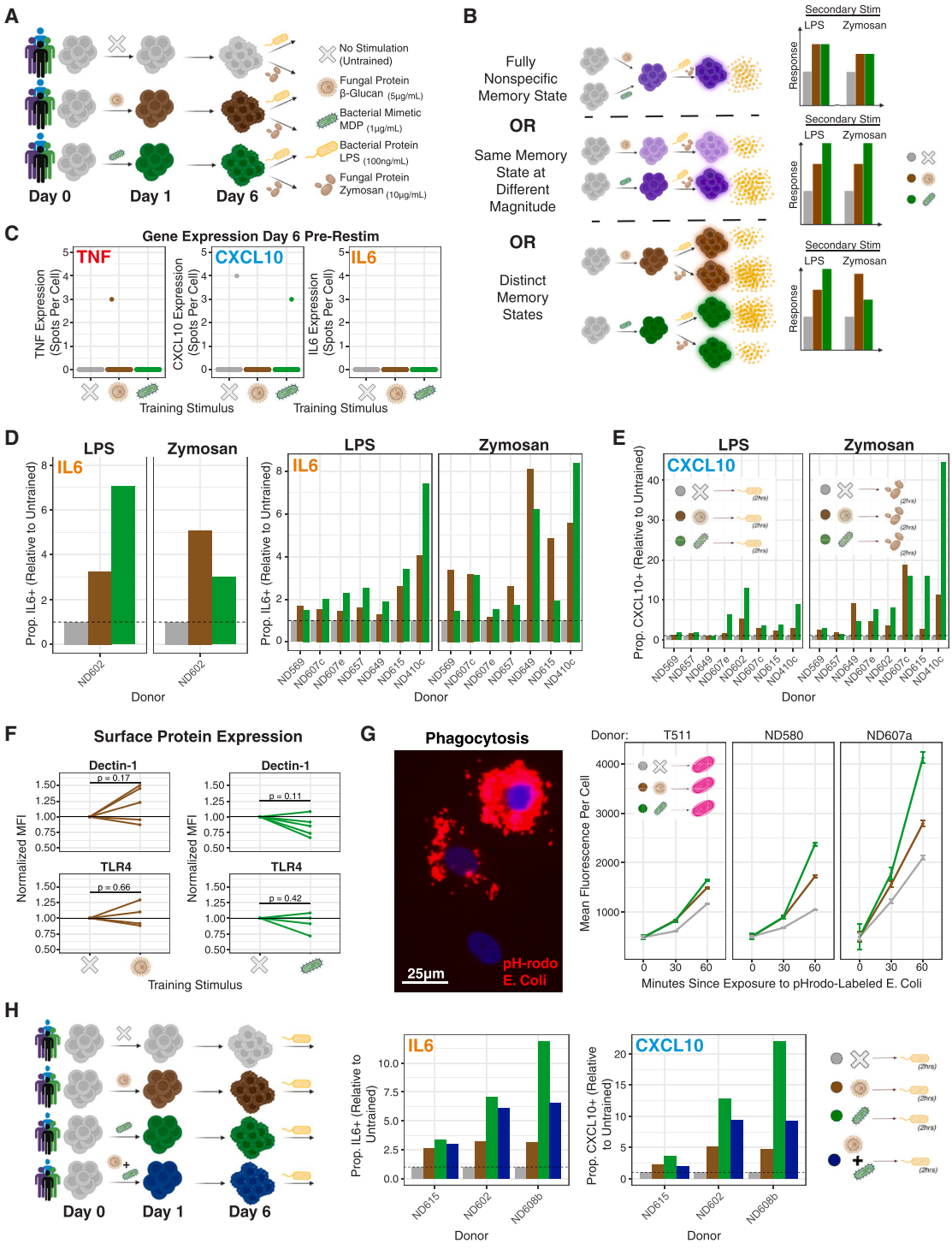

Figure 1. Cells trained with different stimuli mount distinct responses to restimulation

(A) Schematic of experimental procedure. Primary human monocytes were collected from the apheresis product of healthy donors and trained with either 5 μg/mL β-glucan or 1 μg/mL MDP during the first 24 h of culture. On day 6, cells were restimulated with either fungal zymosan (10 μg/mL) or bacterial LPS (100 ng/mL) for 2 h.

(B) Schematic of experimental question and possible results. If β-glucan and MDP training exist on a continuum of a universal training state, then one stimulus should always mount a stronger response to secondary stimulation than the other. If memory states are distinct, different stimuli may mount stronger responses to different secondary stimuli.

(C) Expression of *TNF*, *CXCL10*, and *IL6* assessed by RNA FISH in untrained (gray), β-glucan-trained (brown), and MDP-trained (green) cells on day 6 of culture before restimulation.

(legend continued on next page)

Please cite this article in press as: O'Farrell et al., Human macrophages encode stimulus-specific information of prior exposures through trained immunity, Cell Systems (2026), https://doi.org/10.1016/j.cels.2026.101647

endotoxin tolerance,[4] polarization toward M1 versus M2 states,[32] and memory of stimulation by different classes of interferons,[20,33] are also known to have stimulus-specific outcomes. However, it largely remains unknown whether stimulus-specific training memories affect relevant cellular behaviors, including possible quantitative differences in their responses to different secondary stimulations or differences in memory durability.

Here, we used high-resolution single-cell imaging approaches and bulk epigenetic profiling to identify specificities in trained memory formation and maintenance by two distinct PAMP stimuli (β-glucan and muramyl dipeptide) in primary human monocyte-derived macrophages. We quantified stimulus-specific differences in both the encoding of the trained state into the epigenome and the decoding of this memory into phenotype following restimulation, as well as the durability of these changes over time. Trained cells mounted a stronger response to secondary stimuli more similar to their initial stimulation, suggesting that specificity in the trained state has functional consequences toward future inflammatory responses. Together, our findings demonstrate that specific memory of distinct PAMP exposure is retained at least 6 days following stimulation and that retained specificities of memory influence the response of trained cells to restimulation.

RESULTS

Cells trained with different stimuli mount distinct responses to restimulation

We sought to establish that different training stimuli elicited distinct trained states. We thus first aimed to quantitatively measure phenotypic differences in the trained state that was induced by distinct stimuli, looking for differences in their response to secondary stimulation. We elected to use *in vitro* trained human monocyte-derived macrophages, a commonly used model system for innate immune memory.[4,5,11,22,34] We chose to examine two different primary stimuli in detail: the fungal ligand β-glucan, which is well established to generate trained immunity *in vitro*,[4,35,36] and the bacterial mimetic muramyl dipeptide (MDP), which is thought to mimic the cellular pathways induced through *in vivo* training with the Bacillus Calmette-Guérin (BCG) vaccine.[8,37] β-Glucan and MDP are both commonly used to induce trained immunity (and have both been shown to generate canonical trained phenotypes such as increased *TNF* and *IL6* production), but signal through distinct pathways—as such, comparing the trained responses they generate allowed us to test the hypothesis that memories specific to the primary stimulus can affect the secondary response.

To generate trained cells, we collected monocytes from the apheresis product of healthy donors and stimulated them with the primary stimulus (β-glucan or MDP) for 24 h. Untrained (control) cells received no stimulation during this time. After 24 h, β-glucan or MDP was removed, and the cells were allowed to rest for 5 additional days, during which time they differentiated into monocyte-derived macrophages.[22,35] On day 6, we evaluated the phenotype of these cells, both before and after a secondary stimulation (Figures 1A and 1B). Before secondary stimulation on day 6, trained cells were no longer producing proinflammatory cytokines (Figure 1C; Figure S1A). This reversion to baseline levels of immune activation is archetypal of the trained phenotype, in contrast to priming memory.[3,38]

We wanted to determine what phenotypic differences existed between the trained state of cells with memory of prior β-glucan exposure versus MDP exposure. To this end, we restimulated untrained, β-glucan-trained, and MDP-trained cells with a secondary stimulation of either lipopolysaccharide (LPS, derived from bacteria, as is MDP) or zymosan (derived from fungus, as is β-glucan), with the hypothesis that specificity in the trained state might manifest in a stronger response to a secondary stimulus more similar to the inducing stimulus (Figure 1B).

We found quantifying the proportion of single cells in the population first to express *IL6* or *CXCL10* following restimulation using single-molecule RNA fluorescence *in situ* hybridization (RNA FISH) to be an accurate representation of training within a population of cells exposed to initial stimulation (for more information regarding single-cell quantification of inflammatory gene transcription in trained populations, please see our companion manuscript[39]). As such, we compared the proportion of untrained, β-glucan-trained, and MDP-trained cells expressing *IL6* or *CXCL10* 2 h after stimulation with either LPS or zymosan.

In the majority of donors, we found that β-glucan-trained populations had a greater number of cells expressing *IL6* following stimulation with zymosan (6 of 8 donors), while MDP-trained populations had a greater number of *IL6* expressers following stimulation with LPS (7 of 8 donors) (Figure 1D; Figure S1C). This trend was also somewhat present, although in fewer donors, for *CXCL10* expression (Figure 1E).

These results demonstrate that specific details of a prior inflammatory experience (namely, the identity of the pathogen that was experienced) are retained in trained cells for at least 6 days. These specific memories then influence the magnitude of the inflammatory response induced by secondary stimulation, in a manner dependent on the identity of both the primary and secondary stimuli.

(D and E) Proportion of cells expressing *IL6* or *CXCL10* in untrained (gray), β-glucan-trained (brown), and MDP-trained (green) populations, 2 h after stimulation with either LPS or zymosan. Values were normalized to the untrained value for each donor (indicated by dashed line).
(F) Change in surface protein expression of Dectin-1 and TLR4 between untrained and β-glucan-trained cells (left, brown), and between untrained and MDP-trained cells (right, green), assessed by flow cytometry on day 6 of culture before secondary stimulation.
(G) Left: representative image of fluorescent signal from cells 60 min after stimulation with pH-rodo-labeled *E. coli*. Donor shown is ND580, and the image is representative of 3,100 cells. Right: mean fluorescence per cell (as a metric for amount of phagocytosed particles) over time for untrained (gray), β-glucan-trained (brown), or MDP-trained (green) cells. Error bars reflect the standard error of the mean.
(H) Left: schematic of experimental procedure. Primary human monocytes were collected from the apheresis product of healthy donors and trained with either 5 μg/mL β-glucan, 1 μg/mL MDP, or a combination of 5 μg/mL β-glucan plus 1 μg/mL MDP during the first 24 h of culture. On day 6, cells were restimulated with bacterial LPS for 2 h. Right: proportion of cells expressing *IL6* or *CXCL10* in untrained (gray), β-glucan-trained (brown), MDP-trained (green), or combo-trained (navy) populations, 2 h after stimulation with LPS. Values were normalized to the untrained value for each donor (indicated by dashed line).
Number of single cells analyzed per condition can be found in Table S4.

Please cite this article in press as: O'Farrell et al., Human macrophages encode stimulus-specific information of prior exposures through trained immunity, Cell Systems (2026), https://doi.org/10.1016/j.cels.2026.101647

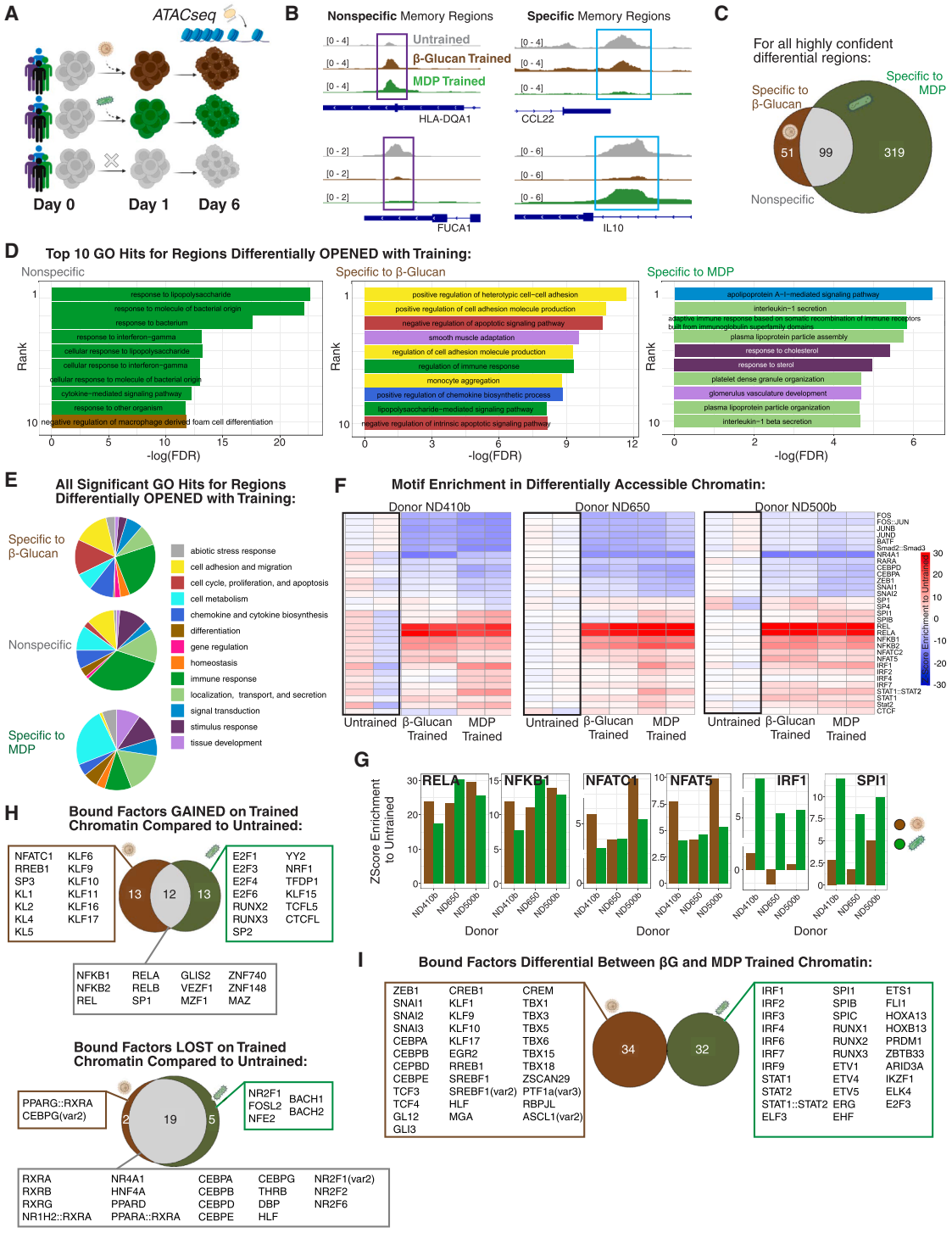

Figure 2. Cells trained with different stimuli have distinct epigenetic profiles

(A) Schematic of experimental procedure. Cells were trained with either β-glucan or MDP on the first day of culture, before resting for 5 days. On day 6, cells were harvested for ATAC-seq to assess chromatin accessibility.

(B) Representative examples of nonspecific (left) and specific (right) memory regions. At nonspecific memory regions, accessibility changed compared with untrained cells in both training conditions. At specific memory regions, accessibility changed compared with untrained cells in one training condition but not the other. BigWig files shown here are merged across technical duplicates, for donor ND410b.

(C) Venn diagram of differential chromatin accessibility in trained cells compared with untrained cells, for regions with high statistical confidence (padj < 0.05 for differential accessibility at that region in at least 2 of 3 donors).

(legend continued on next page)

Please cite this article in press as: O'Farrell et al., Human macrophages encode stimulus-specific information of prior exposures through trained immunity, Cell Systems (2026), https://doi.org/10.1016/j.cels.2026.101647

It is possible that pathogen sensing may partly explain these results. MDP is recognized by the intracellular sensing protein NOD2, while LPS is recognized by surface Toll-like receptor 4 (TLR4). However, zymosan can be recognized by both TLR2 and Dectin-1 receptors (Dectin-1 is the primary receptor that recognizes β-glucan). β-Glucan-trained cells had slightly higher surface Dectin-1 expression, while MDP-trained cells had slightly lower expression, although neither difference was statistically significant (Figure 1F). Neither trained population significantly upregulated TLR4 expression. This result suggests that the increased response to fungal-derived stimuli by cells trained with β-glucan might stem from improved recognition and sensing via upregulation of Dectin-1. However, the limited magnitude of this change suggests improved pathogen sensing may only partly explain these observations.

Macrophages perform many tasks beyond just cytokine and chemokine production. One is phagocytosis, the ability to internalize pathogens. We measured the ability of trained and untrained cells to perform phagocytosis of attenuated *E. coli* conjugated to a dye that fluoresces in the low-pH environment of a phagosome, allowing us to use the fluorescent signal as a readout for phagocytosis efficiency. Both β-glucan-trained and MDP-trained cells had higher mean fluorescence than untrained cells (indicating more efficient phagocytosis), but MDP-trained cells had 1.1–1.5 times stronger fluorescent signal than β-glucan-trained cells 1 h after stimulation (Figure 1G), demonstrating stimulus-specific differences in the functional properties of trained cells beyond immune gene transcription.

Given that training increased the expression of *IL6* and *CXCL10* in a stimulus-specific fashion, we wondered what would occur if we trained cells with a combination of both stimuli simultaneously. We hypothesized that training with both stimuli would lead to even greater expression of these genes following restimulation with LPS than what was observed with single-agent training, as all activating pathways specific to one stimulus would be activated by the combination treatment. Intriguingly, however, we observed an unexpected result: training with both stimuli simultaneously yielded a hybrid phenotype, whereby cells expressed an intermediate amount of *IL6* and *CXCL10* compared with what was seen in populations trained by either stimulus alone (Figure 1H; Figure S1D). This composite phenotype suggests that distinct specific memories can interact within a population of cells in a complex fashion; however, it remains unknown what mechanism could generate such intermediate phenotypes.

Cells trained with different stimuli have distinct epigenetic profiles

We next looked at the epigenome of our trained populations to search for differences in memory "encoding." Because many inflammatory activation pathways (including those initiated by MDP and β-glucan) partly converge upon core signaling factors, we were curious about what molecular differences may exist between retained memories of these different training stimuli.

We performed assay for transposase-accessible chromatin sequencing (ATAC-seq), which measures chromatin accessibility, on monocyte-derived macrophages from three human donors, 6 days after training with a primary stimulus of β-glucan or MDP but before any secondary stimulation (Figure 2A). We compared regions of differential accessibility to untrained cells across these populations to determine whether these differentially accessible "memory regions" were in the same locations (nonspecific memories) or different locations (specific memories) for cells trained with different stimuli.

We identified both specific and nonspecific memory regions in trained cells (Figure 2B). Donor heterogeneity is a known obstacle in the study of trained immunity in primary human samples,[23,24,40] and we observed sizable heterogeneity in the memory regions identified across different donors (Figure S2A). As such, we focused on the 469 memory regions found to be significantly differentially accessible from untrained cells ($p$adj < 0.05) in at least 2 of our 3 sequenced donors (we term these "highly confident" memory regions) (Figure 2C). The majority of highly confident memory regions (86% of β-glucan memory regions and 79% of MDP memory regions) were differentially opened compared with untrained cells (Figure S2B). Of all highly confident memory regions (opened and closed with training), 21% were nonspecific (differentially accessible to untrained in both β-glucan-trained and MDP-trained cells), 11% were specific to β-glucan-trained cells, and 68% were specific to MDP-trained cells.

We next linked our highly confident memory regions to their closest gene and performed Gene Ontology (GO) enrichment analysis[41] (Figures 2D and 2E). For genes nearby regions which opened nonspecifically with training, we found strong enrichment in immune and metabolism-associated pathways, aligning with the wealth of published literature linking trained immunity to metabolic changes.[18,19,42–44] Ontological terms specifically enriched in β-glucan memory regions included cell migration and cell cycle-associated pathways, while those specific to MDP memory regions were enriched in tissue development and metabolic processes.

(D) Top 10 (ordered by statistical significance) Gene Ontology (GO) terms that were nonspecific (left, enriched in both β-glucan-trained and MDP-trained differentially opened chromatin), specific to training with β-glucan (middle), or specific to training with MDP (right) for differentially opened regions of high statistical confidence. Colors reflect the functional category of each term, with the legend shown in (E).

(E) Functional category proportions for all statistically significant (false discovery rate [FDR] < 0.1) GO terms that were nonspecific (middle), specific to β-glucan (top), or specific to MDP (bottom).

(F) Heatmap of differential transcription factor motif accessibility for trained versus untrained samples from each donor, assessed by *chromVAR*. Heatmap colors denote *Z* score enrichment for each motif, with untrained cells from that donor set as the baseline for comparisons.

(G) *Z* score enrichment for accessibility of transcription factor motifs of interest in β-glucan-trained (brown) and MDP-trained (green) chromatin compared with untrained, assessed by *chromVAR*.

(H) Venn diagram of bound factors of high statistical confidence (significantly differential in at least 2 of 3 donors) gained (top) or lost (bottom) on trained chromatin compared with untrained.

(I) Significantly differential bound factors of high statistical confidence (significantly differential in at least 2 of 3 donors) between chromatin of β-glucan-trained cells (brown) and MDP-trained cells (green).

Number of single cells analyzed per condition can be found in Table S4.

Please cite this article in press as: O'Farrell et al., Human macrophages encode stimulus-specific information of prior exposures through trained immunity, Cell Systems (2026), https://doi.org/10.1016/j.cels.2026.101647

We found no specifically enriched GO terms for closed chromatin in β-glucan-trained cells (likely due to the smaller number of identified regions). The one identified nonspecific GO term involved L-serine catabolism, which is known to regulate inflammation.[45] We also identified enrichment in metabolic, developmental, and cell-cell communication-associated ontologies specific to closed chromatin regions in MDP-trained cells (Figure S2C).

Although stimulus-specific differences in the genomic locations of memory-induced epigenetic alterations have been identified in macrophages 24 h after stimulation,[28] we demonstrate here that such specificities of differential chromatin accessibility due to training can be retained in the longer term (at least 6 days) in primary human macrophages.

Next, we used *chromVAR*[46] to perform a motif analysis across all peaks in our trained and untrained samples in an effort to connect differentially accessible chromatin regions to putative transcription factor activity (Figures 2F and 2G). We first looked for transcription factor motifs that were differentially enriched compared with untrained cells across conditions, i.e., nonspecific training motifs. We saw a strong increase in accessibility of motifs associated with NF-κB across all conditions, fitting its canonical role as both a mediator of the inflammatory response and a regulator of chromatin remodeling during inflammation.[47] We also found a strong decrease in accessibility of motifs for transcription factors linked to cell differentiation and immune regulation, including RARA and NR4A1. In 2 of 3 donors, we saw strongly decreased accessibility in regions containing AP-1-associated motifs, including FOS and JUN. Accessibility of AP-1-associated motifs has been shown to increase across many other forms of cellular memory.[48–51] It's possible that the decrease in accessibility of AP-1 motifs observed in this study may be due to the differentiation process from monocyte to macrophage that occurs while in culture, supported by a further decrease in accessibility of these motifs in both trained and untrained cells after 11 days in culture (see Figure 4; Figures S3A and S3B).

We then asked which transcription factor binding sites were more accessible in one trained state than the other. β-Glucan-trained cells showed slightly higher enrichment for NFAT motifs, supported by prior work demonstrating that β-glucan activates NFAT.[52] MDP-trained cells showed greater enrichment in IRF family motifs including IRF1, as well as in macrophage lineage factor SPI1.

We next wanted to determine whether the presence of these differentially accessible motifs might be due to transcription factors still being physically bound to chromatin in trained cells. To do so, we used *TOBIAS*,[53] which identifies regions within peaks of accessible chromatin with lower-than-expected read counts, suggesting that a transcription factor may have been bound at that location at the time of sample collection. We found that bound factors lost in trained populations (i.e., more present on untrained chromatin) were more consistent across different training stimuli, while bound factors gained in trained populations showed more stimulus specificity (Figure 2H). In particular, we saw a nonspecific loss in differentiation-associated factors (including NR4A1 and CEBPD) and a nonspecific gain in NF-κB-associated factors. These results were consistent with our *chromVAR* analysis above, suggesting that differentially accessible motif sequences at least partly reflect the activity of bound transcription factors.

We next directly compared the β-glucan-trained and MDP-trained states to each other to identify putative differentially bound transcription factors between the two trained states (Figure 2I). Both states were enriched for development-associated factors, although from different transcription factor families (β-glucan-trained cells showed greater bound CEBP and TCF family factors, while MDP-trained cells showed greater bound SPI and RUNX family factors). Cells trained with MDP also saw greater enrichment for factors involved in interferon signaling, with several IRF and STAT family factors identified in this analysis. β-Glucan-trained chromatin was enriched for bound factors linked to epithelial-mesenchymal transition (including ZEB1 and SNAI1) and inflammatory regulators (particularly those associated with M2 states, including GLI3,[54] CREB,[55] and EGR2[56]). We also identified differential binding of broadly regulating transcription factor families, including TBOX-family factors enriched on β-glucan-trained chromatin and ETS family factors on MDP-trained chromatin.

We hypothesized that, based on this differential transcription factor binding, β-glucan-trained cells may reflect a more M2-like activation state and MDP-trained cells a more M1-like state. As such, we performed flow cytometry for surface proteins CD80 and CD206, markers associated with M1 and M2 macrophage states, respectively. In 2 of 3 donors, a higher proportion of MDP-trained cells expressed CD80 than both β-glucan-trained cells and untrained cells. In all 3 donors, a higher proportion of β-glucan-trained cells expressed CD206 than both MDP-trained and untrained cells (Figure S2E). These results support the hypothesis that β-glucan-trained cells may exhibit a more M2-like phenotype and MDP-trained cells a more M1-like state.

Differences in chromatin accessibility between cells trained with β-glucan versus MDP were associated with differential activity of transcription factors, with some factors reflecting a generalized training response and others differentially implicated in training with different stimuli. These results suggest different training stimuli activate both shared and specific transcription factors to generate long-term specificities in chromatin accessibility that are retained at least 6 days following training. Future studies may reveal functional connections between these specific transcription factor enrichments and functional activities of trained cells (for instance, enrichment in EMT factors and the migration patterns of trained cells).

Trained cells retain residual active signaling factors 6 days after training

Our ATAC-seq analysis suggested that many immune-activating transcription factors were still actively bound to the chromatin of trained cells more frequently than untrained cells. We wanted to determine whether trained cells also retained active phosphorylated versions of these proteins before restimulation, which would indicate ongoing active signaling through these pathways that might be maintaining chromatin accessibility 6 days after training. It has also been suggested previously that ongoing active signaling may itself encode innate immune memory, such that without continuous ongoing signaling, differentially accessible chromatin regions cannot be maintained.[57]

Please cite this article in press as: O'Farrell et al., Human macrophages encode stimulus-specific information of prior exposures through trained immunity, Cell Systems (2026), https://doi.org/10.1016/j.cels.2026.101647

CellPress

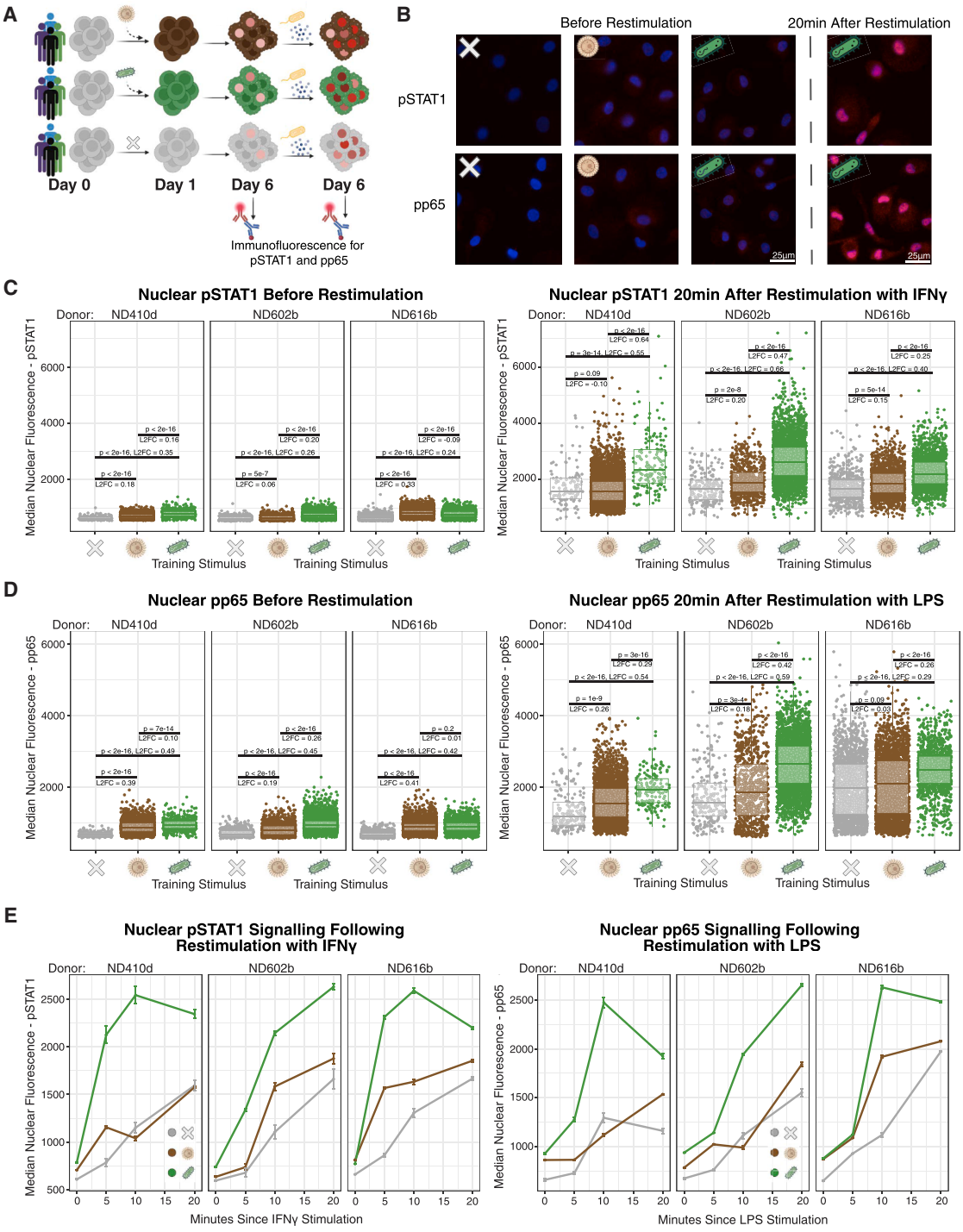

Figure 3. Trained cells retain residual active signaling factors 6 days after training

(A) Schematic of experimental procedure. Cells were trained with either β-glucan or MDP during the first day of culture. On day 6, nuclear phospho-p65 (pp65) and phospho-STAT1 (pSTAT1) were assessed by immunofluorescence either immediately before or 5, 10, or 20 min after stimulation with either LPS at 100 ng/mL (pp65) or IFN-γ at 50 ng/mL (pSTAT1).

(B) Left: representative images of fluorescent pSTAT1 (top) or pp65 (bottom) signal in trained and untrained cells on day 6. Right: representative images of fluorescent pSTAT1 (top) or pp65 (bottom) signal in MDP-trained cells 20 min after stimulation with LPS (pp65) or IFN-γ (pSTAT1). Immunofluorescence signal is contrasted identically across all images. Donor shown is ND602b, and the images are representative of ~1,900 cells per condition.

(legend continued on next page)

Please cite this article in press as: O'Farrell et al., Human macrophages encode stimulus-specific information of prior exposures through trained immunity, Cell Systems (2026), https://doi.org/10.1016/j.cels.2026.101647

As such, we performed immunofluorescence for phospho-p65 (pp65, the RELA subunit of NF-κB) and phospho-STAT1 (pSTAT1) in untrained, β-glucan-trained, and MDP-trained cells 6 days after training (Figures 3A and 3B). Indeed, trained populations showed slightly higher nuclear levels of pp65 and pSTAT1 than their untrained counterparts 6 days after the initial stimulation, suggesting that signaling through these pathways did not fully resolve in this time period (Figures 3C and 3D). MDP-trained cells showed slightly higher pSTAT1 levels than β-glucan-trained cells, but levels were generally comparable between the trained states. However, the magnitude of phosphorylated protein in trained nuclei at this resting state was much lower than what was observed immediately following an acute restimulation (Figures 3C and 3D).

We wondered whether trained cells also re-activated NF-κB and STAT signaling pathways following restimulation faster than untrained cells. We quantified nuclear pp65 5, 10, and 20 min following restimulation with LPS and nuclear pSTAT1 5, 10, and 20 min following restimulation with interferon γ (IFN-γ) (Figure 3E). Despite comparable remnants of phosphorylated pp65 and pSTAT1 in the nuclei of MDP- and β-glucan-trained cells at the resting state, upon restimulation, MDP-trained cells robustly activated both signaling pathways at greater magnitude and speed than either β-glucan-trained or untrained populations. β-Glucan-trained cells activated both signaling pathways at a greater magnitude than seen in untrained populations, but these effects were relatively smaller than what was observed in MDP-trained cells.

Together, these results demonstrate that trained populations retain residual nuclear phosphorylated p65 and STAT1 6 days after training, *despite* cytokine transcription remaining fully off before restimulation. The remnants of signaling pathway activation 6 days after the initial stimulation may be partly responsible for maintaining differential chromatin accessibility in trained cells, allowing for a faster transcriptional response to restimulation. Nuclear pSTAT1 levels before stimulation were higher in MDP-trained than β-glucan-trained populations in 2 of 3 donors, aligning with greater observed chromatin accessibility of STAT motifs in MDP-trained cells.

Durability of the trained state is stimulus specific

Durability, or the longevity of a memory state beyond the initial stimulation, is an important characteristic of trained immunity. Indeed, at longer timescales (beyond 6 days), training memories have been previously shown to be forgotten weeks to months after initial stimulation.[6,8] Our highly controlled, *in vitro* experimental setup allowed us to assess the durability of training memory of a single stimulation event without influence from external signals that might occur *in vivo*. We thus aimed to determine whether the trained state induced by different stimuli differed in its durability (i.e., whether memory of one stimulation was forgotten more quickly than another).

To assess the durability of the encoded state, we performed ATAC-seq on monocyte-derived macrophages from one human donor 6 and 11 days after training with either β-glucan or MDP (Figure 4A). These primary human cells can change state over time while in culture: in an effort to control for these changes, we compared each trained state to an untrained sample taken on the same day (day 6 trained state compared against untrained cells cultured for 6 days; day 11 trained state compared against untrained cells cultured for 11 days) (Figures S3A and S3B).

Although strongly differential on day 6, transcription factor motif enrichment between MDP-trained and untrained cells on day 11 for key inflammatory regulators in the NF-κB family was nearly identical. By contrast, β-glucan-trained cells still retained a strong enrichment of these NF-κB-associated factors in accessible chromatin 11 days after training compared with untrained cells (Figures 4B and 4C). β-glucan-trained cells also had slightly greater nuclear pp65 than MDP-trained cells on day 11 by immunofluorescence, although both trained populations had more pp65 signal than untrained cells (Figure S3C).

We next compared the differential accessibility ($\log_2$ fold change [FC] of accessibility between trained and untrained conditions) of the differentially accessible regions of high statistical confidence identified in Figure 2, for samples sequenced on day 6 versus day 11 (Figure 4D). For MDP-trained cells from this donor, only 1% of highly confident memory regions retained a $\log_2FC > 1$ (compared with 29% of regions on day 6). By contrast, for β-glucan-trained cells, 25% of these regions retained a $\log_2FC > 1$ (compared with 39% on day 6). Thus, chromatin accessibility changes generated by training with β-glucan appear to be maintained for a longer period of time compared with those generated by training with MDP, suggesting β-glucan generates a more durable memory in macrophages *in vitro*.

These results were supported by a decreased transcriptional response to restimulation with LPS in MDP-trained cells 11 days following training (Figure 4E). Six days after training, MDP-trained cells showed the strongest activation of *IL6* expression following LPS restimulation. However, 11 days after training, the MDP-trained population expressed *IL6* at levels more similar to untrained populations, while β-glucan-trained cells retained their boosted expression compared with untrained cells.

These findings suggest that the trained state generated by β-glucan stimulation is more durable than that generated by MDP stimulation *in vitro*. As such, we can identify durability as another facet of trained innate immune memory that is stimulus specific, as memory of certain training stimuli appears to last longer than others.

Stimulus specificity of trained states extends beyond β-glucan and MDP

β-Glucan and MDP are commonly used to induce trained immunity, but many other stimuli can also be used to train macrophages. Having identified specificities in the trained states induced by β-glucan and MDP, we next wanted to compare

(C and D) Median nuclear fluorescent signal per cell for pSTAT1 or pp65 in untrained (gray), β-glucan-trained (brown), or MDP-trained (green) cells, on day 6 before (left) or 20 min after (right) stimulation.

(E) Time course of pSTAT1 (left) and pp65 (right) nuclear fluorescent intensity 0, 5, 10, and 20 min following stimulation with LPS (pp65) or IFN-γ (pSTAT1) in untrained (gray), β-glucan-trained (brown) or MDP-trained (green) cells. Error bars reflect the standard error of the mean.

Number of single cells analyzed per condition can be found in Table S4.

Please cite this article in press as: O'Farrell et al., Human macrophages encode stimulus-specific information of prior exposures through trained immunity, Cell Systems (2026), https://doi.org/10.1016/j.cels.2026.101647

CellPress

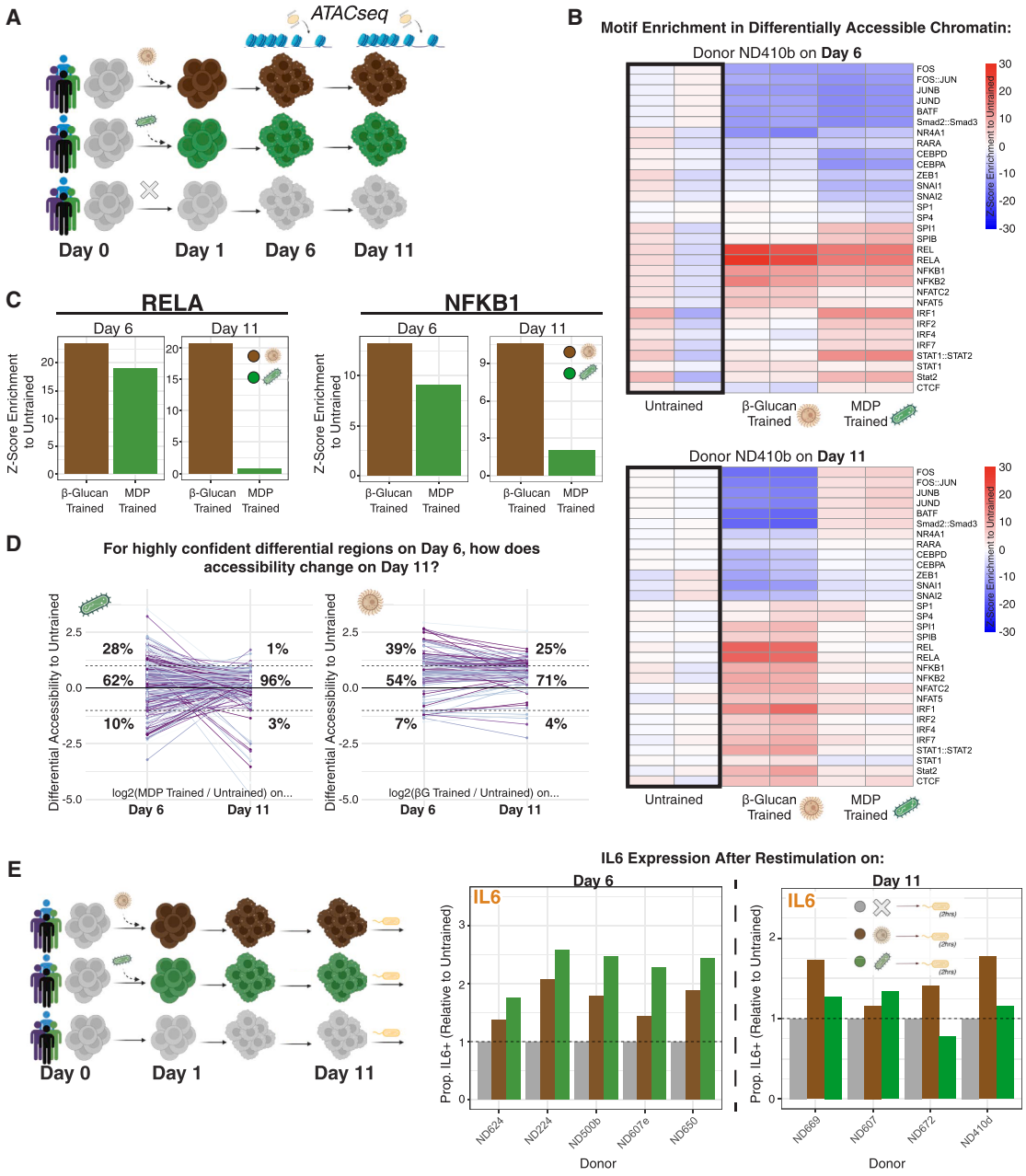

Figure 4. Durability of the trained state is stimulus specific

(A) Schematic of experimental procedure. Cells from one donor were trained with either β-glucan or MDP on the first day of culture. On days 6 and 11, cells were harvested for ATAC-seq to assess chromatin accessibility.

(B) Heatmap of differential transcription factor motif analysis for trained versus untrained samples on day 6 (top) and day 11 (bottom) of culture. Heatmap colors denote *Z* score enrichment for each motif, with untrained cells from that time point set as the baseline for comparisons.

(C) *Z* score enrichment for accessibility of transcription factor motifs RELA and NFKB1 in chromatin from β-glucan-trained cells (brown) and MDP-trained cells (green) on days 6 and 11 of culture, compared with untrained cells from that time point.

(D) Comparison of $\log_2$FC of chromatin accessibility for regions deemed highly confident memory regions ($p$adj < 0.05 for differential accessibility trained versus untrained in at least 2 of 3 donors on day 6, as shown in Figure 2C) on day 6 versus day 11. Each colored line represents one differential region.

(E) Left: schematic of experimental procedure. Cells were trained with either β-glucan or MDP on the first day of culture, then stimulated with 100 ng/mL LPS for 2 h on either days 6 or 11. Right: proportion of cells expressing *IL6* in untrained (gray), β-glucan-trained (brown), and MDP-trained (green) populations 2 h after stimulation with LPS on day 6 versus day 11 of culture, normalized to the untrained value for each donor (indicated by dashed line). Note: the same donors are not shown across both time points.

Number of single cells analyzed per condition can be found in Table S4.

Please cite this article in press as: O'Farrell et al., Human macrophages encode stimulus-specific information of prior exposures through trained immunity, Cell Systems (2026), https://doi.org/10.1016/j.cels.2026.101647

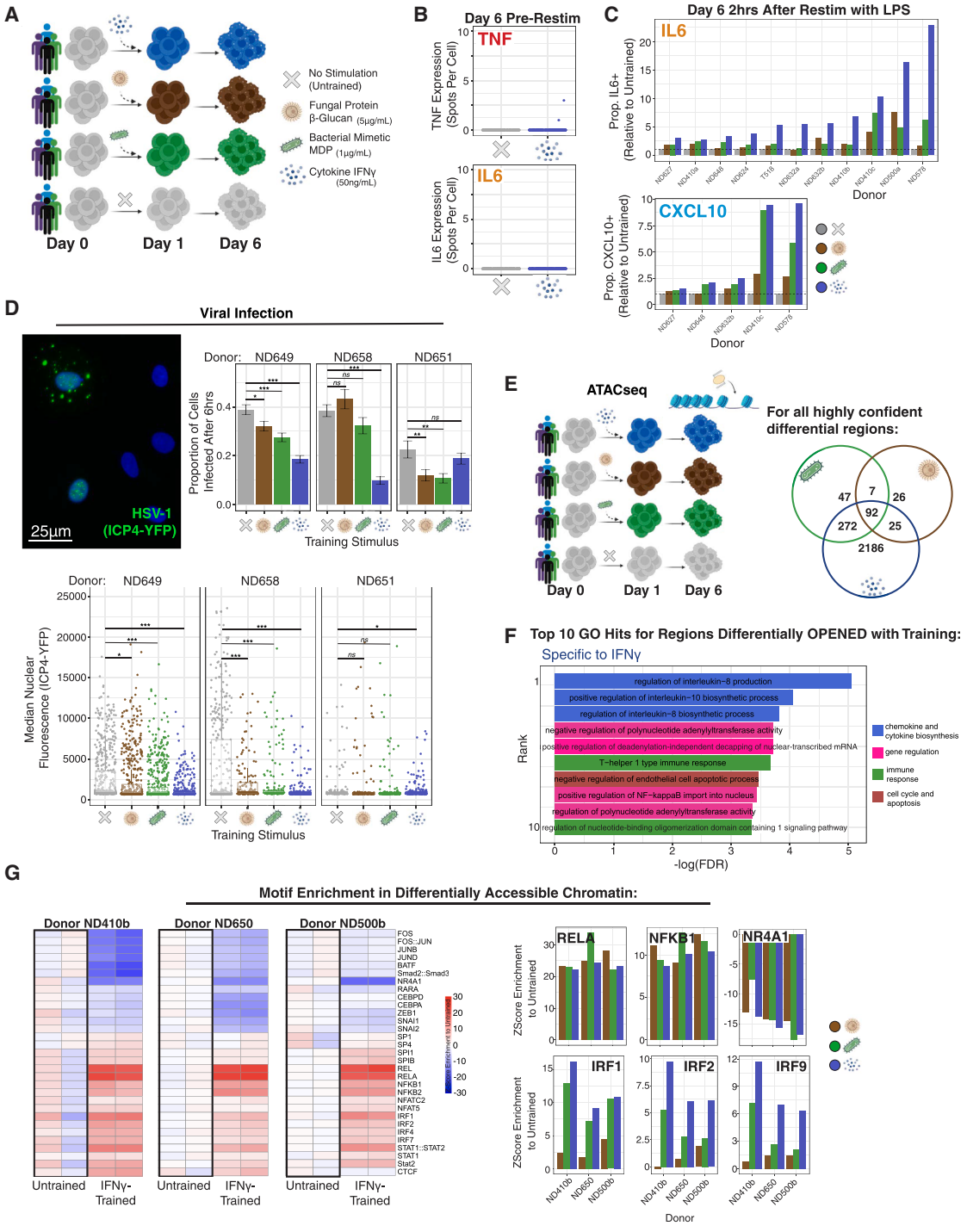

Figure 5. Stimulus specificity of trained states extends beyond β-glucan and MDP

(A) Schematic of experimental procedure. Cells were trained with either fungal protein β-glucan, bacterial mimetic MDP, or cytokine IFN-γ for the first 24 h of culture. On day 6, trained and untrained cells were assessed.

(B) Expression of *TNF* and *IL6* assessed by RNA FISH in untrained (gray) and IFN-γ-trained (blue) cells on day 6 of culture before restimulation.

(C) Proportion of cells expressing *IL6* or *CXCL10* in untrained (gray), β-glucan-trained (brown), MDP-trained (green), and IFN-γ-trained (blue) populations 2 h after stimulation with LPS, normalized by value from the untrained sample (indicated by dashed horizontal line).

(D) Top left: representative image of fluorescent signal from cells 6 h after challenge with fluorescently labeled HSV-1. Early-stage infection shows diffuse nuclear fluorescent signal, while later-stage infection shows punctated signal in the cytoplasm. Donor shown is ND649, and the image is representative of ~600 cells per condition. Top right: proportion of cells infected in untrained (gray), β-glucan-trained (brown), MDP-trained (green), and IFN-γ-trained (blue) populations 6 h after viral challenge. Error bars show the standard error of percentage. Bottom: median nuclear fluorescence (as a proxy for degree of infection) in untrained (gray),

(legend continued on next page)

these states to those induced by other stimuli, to determine how specificity manifested across a wider range of training stimuli.

We first focused our efforts on the host-derived proinflammatory cytokine IFN-γ, which is known to alter macrophage state at short timescales (24–48 h, via priming[28,58,59]). We wanted to determine whether memory of IFN-γ stimulation was still present at longer timescales (6–11 days after stimulation) and whether this longer-term memory resembled training (where inflammatory responses return to baseline) or priming (where immune response genes retain some active transcription)[3] (Figure 5A). Six days after stimulation with IFN-γ, monocyte-derived macrophages did not express proinflammatory cytokines *TNF* or *IL6* and resolved pp65 and pSTAT1 signaling to approximately the same level as β-glucan-trained and MDP-trained cells (Figure 5B; Figure S4A). As such, we considered this longer-term memory of IFN-γ exposure to be a training memory.

Cells trained with IFN-γ expressed *IL6* and *CXCL10* at much greater levels than untrained cells (and greater than what was achieved by β-glucan or MDP training) 2 h after restimulation with LPS (Figure 5C; Figure S4B). Because IFN-γ signaling is known to disrupt viral replication,[60–62] we tested whether trained cells were less susceptible to infection with virus, with the hypothesis that IFN-γ-trained cells would be the least likely to be infected. We used a live, replicating herpes simplex virus 1 (HSV-1) with a fluorescent tag on ICP4, a protein involved in viral replication.[63] Results were variable across donors, but we generally found that training slightly reduced the proportion of cells infected by HSV-1 (by approximately 6%–11%), with IFN-γ-trained cells being the least infected in 2 of 3 donors (Figure 5D).

By ATAC-seq, we identified 2,575 highly confident differentially accessible regions in chromatin from IFN-γ-trained cells compared with untrained cells (Figure 5E). The majority of these highly confident memory regions (85%) were specific to IFN-γ-trained cells and not differentially accessible in cells trained with β-glucan or MDP. Notably, the vast majority (93%) of shared differential regions between β-glucan-trained and MDP-trained cells were also shared with IFN-γ-trained cells, suggesting they reflect a true nonspecific "core" of epigenetic changes linked to training. Unlike what was observed in highly confident regions from β-glucan-trained or MDP-trained cells, approximately half (46%) of highly confident memory regions in IFN-γ-trained cells were differentially closed compared with untrained cells.

Top specific GO hits for regions opened in IFN-γ-trained cells include regulation of interleukin (IL)-8 and IL-10 production (Figure 5F). Chromatin from IFN-γ-trained cells showed increased accessibility at regions with NF-κB-associated transcription factor motifs (at comparable levels to β-glucan- and MDP-trained cells), as well as IRF family motifs (Figure 5G). Differential accessibility of these transcription factor motifs was retained 11 days after training (Figure S4C), indicating durable memory *in vitro*.

In one additional donor, we performed ATAC-seq on cells 6 days after stimulation with CpG, poly(I:C), oxidized low-density lipoprotein (oxLDL), or transforming growth factor β (TGF-β). We also identified stimulus-specific regions of accessible chromatin and transcription factor motif accessibility (Figures S5A and S5B). oxLDL and TGF-β-trained cells showed a reduction in NF-κB-associated motifs, while cells trained with poly(I:C) showed strong enrichment for SPI, IRF, and STAT motifs but not NF-κB motifs. Cells trained with CpG showed very limited differences in chromatin accessibility compared with untrained cells.

Together, these results suggest multiple training agents (not solely β-glucan and MDP) generate distinct trained states that may influence the phenotypic outcome of memory and that IFN-γ in particular generates potent, long-term training memory.

DISCUSSION

Here, we provide a highly quantitative measure of the specificity of training memory in primary human monocyte-derived macrophages. Specificity in the trained state exists within epigenetic, transcriptomic, proteomic, and signaling compartments of a trained macrophage. In the future, such specificities may be exploited for therapeutic purposes by selecting a particular training agent to generate a specific trained state with desired properties of interest (for instance, selecting an agent that generates a trained state with strongest response against a pathogen of interest, or one that builds the most durable memory, as some examples).

Although we make distinctions between training and priming memories based on transcriptional activation of immune response genes (namely, that a lack of transcription of *TNF*, *IL6*, or *CXCL10* before restimulation on day 6 indicates these are "trained" cells in a quiescent state), we note that cells that experienced β-glucan, MDP, or IFN-γ in their past are still notably distinct from untrained cells before restimulation. For instance, if we defined a "return to baseline" following initial stimulation by phosphorylated signaling proteins or by surface protein expression, we might consider these cells "primed" rather than trained. When defining innate immune memory phenotypes, we believe it is important to identify the compartments of storage of these memories within the cell and to delineate where changes have occurred following the initial stimulation and where such changes are maintained in the resting state of the cell.

β-glucan-trained (brown), MDP-trained (green), and IFN-γ-trained (blue) populations 6 h after viral challenge. Statistics: ***$p < 0.001$, **$p < 0.01$, *$p < 0.05$, NS $p > 0.05$.

(E) Left: schematic of experimental procedure. Cells from 3 donors were trained with either fungal protein β-glucan, bacterial mimetic MDP, or host cytokine IFN-γ for the first 24 h of culture. On day 6, cells were harvested for ATAC-seq. Right: Venn diagram of chromatin accessibility in trained cells compared with untrained cells, for differential regions with high statistical confidence ($p$adj < 0.05 in at least 2 of 3 donors).

(F) Top 10 (ordered by statistical significance) GO terms for highly confident differentially opened regions that were specific to training with IFN-γ. Colors reflect the functional category of each term.

(G) Left: heatmap of differential transcription factor motif accessibility for IFN-γ-trained versus untrained samples from each donor, assessed by *chromVAR*. Heatmap colors denote *Z* score enrichment for each motif, with untrained cells from that donor set as the baseline for comparisons. Right: *Z* score enrichment for accessibility of transcription factor motifs of interest, in β-glucan-trained (brown), MDP-trained (green), and IFN-γ-trained (blue) populations.

Number of single cells analyzed per condition can be found in Table S4.

We demonstrate specificity of trained states in an isolated, *in vitro* setup. It's possible that specific memories may be overwritten by new environmental cues from other cells in an *in vivo* setting, potentially changing the magnitude or appearance of memory specificity. Training *in vivo* can also manifest as changes to bone-marrow-derived progenitor cells—something we are unable to model in this system—which likely influences memory phenotype and durability. In a tissue context, remembered signals also likely occur in combination, making specificities challenging to disentangle. Indeed, as we found when combining training stimuli, memories of multiple stimuli appear to interact in a complex fashion. Spatial cues may also play a role in memory formation and maintenance, as signal gradients and neighboring cells likely influence what exactly is remembered by each individual cell.

It is known that macrophages dynamically tune their activation state according to a complex network of environmental stimuli, providing context-adjusted responses to stimulation.[64,65] We suggest that specific memories of prior stimulation (not only memory of activation but also of the *type* of activation) also play an important role in macrophage phenotype. Binary categories of M1 and M2 macrophages are increasingly viewed as an oversimplification of complex activation states, which can vary widely based on stimulation type and time.[32] Classification schemas that reference memory of a specific stimulus may improve the accuracy and reproducibility of reported macrophage signatures.

Macrophage memory has been shown to be reversible when cells are challenged with a new stimulus.[4,66,67] It remains unknown whether memories of certain stimuli may be more or less mutable. In an *in vitro* setting, we show that memory can persist in primary monocyte-derived macrophages for at least 11 days. Although enhanced cytokine and chemokine production from these memories may be useful in fighting pathogens, the accumulation of deleterious memories may influence phenotypes like chronic inflammation. As such, disentangling stimulus specificities of these memories may unlock vital clues toward generating or removing innate immune memories for therapeutic benefit.

RESOURCE AVAILABILITY

Lead contact

Requests should be directed to and will be fulfilled by the lead contact, Arjun Raj (arjunrajlab@gmail.com).

Materials availability

This study did not generate any new reagents.

Data and code availability

- Bulk ATAC-seq data generated in this study have been deposited to GEO under accession number GEO: GSE323311.
- All code used to analyze data and generate figures can be found on Dropbox at https://www.dropbox.com/scl/fo/q5jt87fhviyv4ytgvgpqt/AObPxhHcmDGD6RixA8Z7NQE?rlkey=sfqf8w9wewcq1zlte6xbueixo&st=d0m469u5&dl=0 and on Data Dryad at https://doi.org/10.5061/dryad.stqjq2cjc and is publicly available as of the date of this publication.
- Any additional information required to reanalyze the data reported in this paper is available from the lead contact upon request.

ACKNOWLEDGMENTS

The authors would like to thank members of the Raj Lab for scientific discussion and detailed commentary on the manuscript, in particular Serena El Feghali, Pavithran Ravindran, Grant Kinsler, Gianna Busch, and Catherine Triandafillou; Professor Sunny Shin for expert guidance on macrophage biology; Dr. Shuo Zhang from the Penn Epigenetics Institute, as well as Raj Lab members Vinay Ayyappan and Miles Arnett, for assistance with computational analysis of ATAC-seq data; summer research students Juan McCook and Nava Graham for scientific discussion and collaborative efforts; the Genomics Sequencing Core at the Wistar Institute, in particular Sonali Majumdar and Sandy Widura, for assistance with sequencing; Professor Nir Drayman for the kind gift of the HSV1-YCP4 virus; and the William Greenleaf lab for providing custom primer sequences used in ATAC-seq experiments. Figure cartoons were created using Biorender.com.

The authors thank Emily Cento, Zhilin Chen, Max A. Eldabbas, and Emileigh Maddox of the Human Immunology Core and the Division of Transfusion Medicine and Therapeutic Pathology at the Perelman School of Medicine at the University of Pennsylvania for providing de-identified monocytes that were purified from healthy donor apheresis using StemCell RosetteSep kits. The HIC is supported in part by NIH P30 AI045008 and P30 CA016520. HIC RRID: SCR_022380.

Cytomics data for this manuscript were generated using the Penn Cytomics and Cell Sorting Shared Resource Laboratory at the University of Pennsylvania (RRID: SCR_022376). Penn Cytomics is partially supported by the Abramson Cancer Center NCI grant P30 016520.

A.R. acknowledges support from a center grant from the Mark Foundation for Cancer Research and NIH Director's Transformative Research Award R01 GM137425. This project was made possible through the support of grant 63532 from the John Templeton Foundation. A.O. acknowledges support from NSF GRFP DGE-2236662. Z.N. acknowledges support from the Roy and Diana Vagelos Scholars Program in the Molecular Life Sciences, the Roy and Diana Vagelos Science Challenge Award, the Barry M. Goldwater Scholarship, the Fannie and John Hertz Foundation Fellowship, the Paul & Daisy Soros Fellowship for New Americans, and the Department of Energy Computational Science Graduate Fellowship. J.L. acknowledges support from NIH Medical Scientist Training Program T32GM007170.

AUTHOR CONTRIBUTIONS

A.O. and A.R. conceived the project and designed all experiments. Z.N. and A.R. developed image analysis software for all image analyses used in this manuscript, including automated RNA FISH spot detection. J.L. assisted A.O. with ATAC-seq experiments. L.C.V.E. assisted A.O. with viral infection and flow cytometry experiments. K.S. provided the Tn5 enzyme used in ATAC-seq experiments. A.O. and A.R. prepared all illustrations and wrote the manuscript, with input from all authors.

DECLARATION OF INTERESTS

A.R. receives royalties related to Stellaris RNA FISH probes. A.R. serves on the scientific advisory board of Spatial Genomics and is an employee of Somite Therapeutics while on sabbatical leave.

DECLARATION OF GENERATIVE AI AND AI-ASSISTED TECHNOLOGIES IN THE WRITING PROCESS

During the preparation of this work, the authors used Claude to generate and comment code for analyses. After using this tool or service, the authors reviewed and edited the content and take full responsibility for the content of the publication.

STAR★METHODS

Detailed methods are provided in the online version of this paper and include the following:

- KEY RESOURCES TABLE

SUPPLEMENTAL INFORMATION

Supplemental information can be found online at https://doi.org/10.1016/j.cels.2026.101647.

Received: January 31, 2025
Revised: October 20, 2025
Accepted: May 27, 2026

REFERENCES

1. Netea, M.G., Joosten, L.A.B., Latz, E., Mills, K.H.G., Natoli, G., Stunnenberg, H.G., O'Neill, L.A.J., and Xavier, R.J. (2016). Trained immunity: A program of innate immune memory in health and disease. Science *352*, aaf1098. https://doi.org/10.1126/science.aaf1098.
2. Netea, M.G., Domínguez-Andrés, J., Barreiro, L.B., Chavakis, T., Divangahi, M., Fuchs, E., Joosten, L.A.B., van der Meer, J.W.M., Mhlanga, M.M., Mulder, W.J.M., et al. (2020). Defining trained immunity and its role in health and disease. Nat. Rev. Immunol. *20*, 375–388. https://doi.org/10.1038/s41577-020-0285-6.
3. Divangahi, M., Aaby, P., Khader, S.A., Barreiro, L.B., Bekkering, S., Chavakis, T., van Crevel, R., Curtis, N., DiNardo, A.R., Dominguez-Andres, J., et al. (2021). Trained immunity, tolerance, priming and differentiation: distinct immunological processes. Nat. Immunol. *22*, 2–6. https://doi.org/10.1038/s41590-020-00845-6.
4. Novakovic, B., Habibi, E., Wang, S.-Y., Arts, R.J.W., Davar, R., Megchelenbrink, W., Kim, B., Kuznetsova, T., Kox, M., Zwaag, J., et al. (2016). β-Glucan Reverses the Epigenetic State of LPS-Induced Immunological Tolerance. Cell *167*, 1354–1368.e14. https://doi.org/10.1016/j.cell.2016.09.034.
5. Ifrim, D.C., Quintin, J., Joosten, L.A.B., Jacobs, C., Jansen, T., Jacobs, L., Gow, N.A.R., Williams, D.L., van der Meer, J.W.M., and Netea, M.G. (2014). Trained immunity or tolerance: opposing functional programs induced in human monocytes after engagement of various pattern recognition receptors. Clin. Vaccine Immunol. *21*, 534–545. https://doi.org/10.1128/CVI.00688-13.
6. Adamson, M.S., Nesic, S., Buness, A., Bayrak, K., Schmitz, S., Soler, S., Zillinger, T., Marx, S., Lambing, S., Andryka-Cegielski, K., et al. (2022). RIG-I activation primes and trains innate antiviral immune memory. Preprint at bioRxiv. https://doi.org/10.1101/2022.10.27.514004.
7. Murphy, D.M., Cox, D.J., Connolly, S.A., Breen, E.P., Brugman, A.A., Phelan, J.J., Keane, J., and Basdeo, S.A. (2023). Trained immunity is induced in humans after immunization with an adenoviral vector COVID-19 vaccine. J. Clin. Invest. *133*, e162581. https://doi.org/10.1172/JCI162581.
8. Kong, L., Moorlag, S.J.C.F.M., Lefkovith, A., Li, B., Matzaraki, V., van Emst, L., Kang, H.A., Latorre, I., Jaeger, M., Joosten, L.A.B., et al. (2021). Single-cell transcriptomic profiles reveal changes associated with BCG-induced trained immunity and protective effects in circulating monocytes. Cell Rep. *37*, 110028. https://doi.org/10.1016/j.celrep.2021.110028.
9. Kaufmann, E., Khan, N., Tran, K.A., Ulndreaj, A., Pernet, E., Fontes, G., Lupien, A., Desmeules, P., McIntosh, F., Abow, A., et al. (2022). BCG vaccination provides protection against IAV but not SARS-CoV-2. Cell Rep. *38*, 110502. https://doi.org/10.1016/j.celrep.2022.110502.
10. Cheong, J.-G., Ravishankar, A., Sharma, S., Parkhurst, C.N., Grassmann, S.A., Wingert, C.K., Laurent, P., Ma, S., Paddock, L., Miranda, I.C., et al. (2023). Epigenetic memory of coronavirus infection in innate immune cells and their progenitors. Cell *186*, 3882–3902.e24. https://doi.org/10.1016/j.cell.2023.07.019.
11. Carlile, S.R., Cahill, S.C., O'Brien, E.C., Neto, N.G.B., Monaghan, M.G., and McLoughlin, R.M. (2024). Staphylococcus aureus induced trained immunity in macrophages confers heterologous protection against gram-negative bacterial infection. iScience *27*, 111284. https://doi.org/10.1016/j.isci.2024.111284.
12. Bekkering, S., Quintin, J., Joosten, L.A.B., van der Meer, J.W.M., Netea, M.G., and Riksen, N.P. (2014). Oxidized low-density lipoprotein induces long-term proinflammatory cytokine production and foam cell formation via epigenetic reprogramming of monocytes. Arterioscler. Thromb. Vasc. Biol. *34*, 1731–1738. https://doi.org/10.1161/ATVBAHA.114.303887.
13. van der Heijden, C.D.C.C., Groh, L., Keating, S.T., Kaffa, C., Noz, M.P., Kersten, S., van Herwaarden, A.E., Hoischen, A., Joosten, L.A.B., Timmers, H.J.L.M., et al. (2020). Catecholamines induce trained immunity in monocytes in vitro and in vivo. Circ. Res. *127*, 269–283. https://doi.org/10.1161/CIRCRESAHA.119.315800.
14. Naik, S., Larsen, S.B., Gomez, N.C., Alaverdyan, K., Sendoel, A., Yuan, S., Polak, L., Kulukian, A., Chai, S., and Fuchs, E. (2017). Inflammatory memory sensitizes skin epithelial stem cells to tissue damage. Nature *550*, 475–480. https://doi.org/10.1038/nature24271.
15. Nakayama, Y., Fujiu, K., Oshima, T., Matsuda, J., Sugita, J., Matsubara, T.J., Liu, Y., Goto, K., Kani, K., Uchida, R., et al. (2024). Heart failure promotes multimorbidity through innate immune memory. Sci. Immunol. *9*, eade3814. https://doi.org/10.1126/sciimmunol.ade3814.
16. Di Luzio, N.R., and Williams, D.L. (1978). Protective effect of glucan against systemic Staphylococcus aureus septicemia in normal and leukemic mice. Infect. Immun. *20*, 804–810. https://doi.org/10.1128/iai.20.3.804-810.1978.
17. Arts, R.J.W., Moorlag, S.J.C.F.M., Novakovic, B., Li, Y., Wang, S.-Y., Oosting, M., Kumar, V., Xavier, R.J., Wijmenga, C., Joosten, L.A.B., et al. (2018). BCG vaccination protects against experimental viral infection in humans through the induction of cytokines associated with trained immunity. Cell Host Microbe *23*, 89–100.e5. https://doi.org/10.1016/j.chom.2017.12.010.
18. Domínguez-Andrés, J., Novakovic, B., Li, Y., Scicluna, B.P., Gresnigt, M.S., Arts, R.J.W., Oosting, M., Moorlag, S.J.C.F.M., Groh, L.A., Zwaag, J., et al. (2019). The Itaconate Pathway Is a Central Regulatory Node Linking Innate Immune Tolerance and Trained Immunity. Cell Metab. *29*, 211–220.e5. https://doi.org/10.1016/j.cmet.2018.09.003.
19. Fanucchi, S., Domínguez-Andrés, J., Joosten, L.A.B., Netea, M.G., and Mhlanga, M.M. (2021). The Intersection of Epigenetics and Metabolism in Trained Immunity. Immunity *54*, 32–43. https://doi.org/10.1016/j.immuni.2020.10.011.
20. Chen, L., and Ozato, K. (2021). Innate immune memory in hematopoietic stem/progenitor cells: Myeloid-biased differentiation and the role of interferon. Front. Immunol. *12*, 621333. https://doi.org/10.3389/fimmu.2021.621333.
21. Sun, S., Aguirre-Gamboa, R., and Barreiro, L.B. (2023). Transmission of stimulus-induced epigenetic changes through cell division is coupled to continuous transcription factor activity. Front. Immunol. *14*, 1129577. https://doi.org/10.3389/fimmu.2023.1129577.
22. Bekkering, S., Blok, B.A., Joosten, L.A.B., Riksen, N.P., van Crevel, R., and Netea, M.G. (2016). In Vitro Experimental Model of Trained Innate Immunity in Human Primary Monocytes. Clin. Vaccine Immunol. *23*, 926–933. https://doi.org/10.1128/CVI.00349-16.
23. Messina, N.L., Netea, M.G., and Curtis, N. (2020). The impact of human single nucleotide polymorphisms on Bacillus Calmette-Guérin responses. Vaccine *38*, 6224–6235. https://doi.org/10.1016/j.vaccine.2020.07.032.
24. Moorlag, S.J.C.F.M., Folkman, L., ter Horst, R., Krausgruber, T., Barreca, D., Schuster, L.C., Fife, V., Matzaraki, V., Li, W., Reichl, S., et al. (2024). Multi-omics analysis of innate and adaptive responses to BCG vaccination

reveals epigenetic cell states that predict trained immunity. Immunity *57*, 171–187.e14. https://doi.org/10.1016/j.immuni.2023.12.005.

25. Knight, H.R., Ketter, E., Ung, T., Weiss, A., Ajit, J., Chen, Q., Shen, J., Ip, K.M., Chiang, C.-Y., Barreiro, L., et al. (2024). High-throughput screen identifies non inflammatory small molecule inducers of trained immunity. Proc. Natl. Acad. Sci. USA *121*, e2400413121. https://doi.org/10.1073/pnas.2400413121.
26. Xu, J.-C., Chen, Z.-Y., Huang, X.-J., Wu, J., Huang, H., Niu, L.-F., Wang, H.-L., Li, J.-H., Lowrie, D.B., Hu, Z., et al. (2024). Multi-omics analysis reveals that linoleic acid metabolism is associated with variations of trained immunity induced by distinct BCG strains. Sci. Adv. *10*, eadk8093. https://doi.org/10.1126/sciadv.adk8093.
27. Cheng, Q.J., Farrell, K., Fenn, J., Ma, Z., Makanani, S.K., and Siemsen, J. (2024). Dectin-1 ligands produce distinct training phenotypes in human monocytes through differential activation of signaling networks. Sci. Rep. *14*, 1454. https://doi.org/10.1038/s41598-024-51620-8.
28. Ostuni, R., Piccolo, V., Barozzi, I., Polletti, S., Termanini, A., Bonifacio, S., Curina, A., Prosperini, E., Ghisletti, S., and Natoli, G. (2013). Latent enhancers activated by stimulation in differentiated cells. Cell *152*, 157–171. https://doi.org/10.1016/j.cell.2012.12.018.
29. Cheng, Q.J., Ohta, S., Sheu, K.M., Spreafico, R., Adelaja, A., Taylor, B., and Hoffmann, A. (2021). NF-κB dynamics determine the stimulus specificity of epigenomic reprogramming in macrophages. Science *372*, 1349–1353. https://doi.org/10.1126/science.abc0269.
30. Butcher, S.K., O'Carroll, C.E., Wells, C.A., and Carmody, R.J. (2018). Toll-Like Receptors Drive Specific Patterns of Tolerance and Training on Restimulation of Macrophages. Front. Immunol. *9*, 933. https://doi.org/10.3389/fimmu.2018.00933.
31. Kamada, R., Yang, W., Zhang, Y., Patel, M.C., Yang, Y., Ouda, R., Dey, A., Wakabayashi, Y., Sakaguchi, K., Fujita, T., et al. (2018). Interferon stimulation creates chromatin marks and establishes transcriptional memory. Proc. Natl. Acad. Sci. USA *115*, E9162–E9171. https://doi.org/10.1073/pnas.1720930115.
32. Strizova, Z., Benesova, I., Bartolini, R., Novysedlak, R., Cecrdlova, E., Foley, L.K., and Striz, I. (2023). M1/M2 macrophages and their overlaps - myth or reality? Clin. Sci. (Lond.) *137*, 1067–1093. https://doi.org/10.1042/CS20220531.
33. Khan, N., Downey, J., Sanz, J., Kaufmann, E., Blankenhaus, B., Pacis, A., Pernet, E., Ahmed, E., Cardoso, S., Nijnik, A., et al. (2020). M. tuberculosis Reprograms Hematopoietic Stem Cells to Limit Myelopoiesis and Impair Trained Immunity. Cell *183*, 752–770.e22. https://doi.org/10.1016/j.cell.2020.09.062.
34. Zhang, B., Moorlag, S.J., Domínguez-Andrés, J., Bulut, Ö., Kilic, G., Liu, Z., van Crevel, R., Xu, C.-J., Joosten, L.A., Netea, M.G., et al. (2022). Single-cell RNA sequencing reveals induction of distinct trained-immunity programs in human monocytes. J. Clin. Invest. *132*, e147719. https://doi.org/10.1172/JCI147719.
35. Saeed, S., Quintin, J., Kerstens, H.H.D., Rao, N.A., Aghajanirefah, A., Matarese, F., Cheng, S.-C., Ratter, J., Berentsen, K., van der Ent, M.A., et al. (2014). Epigenetic programming of monocyte-to-macrophage differentiation and trained innate immunity. Science *345*, 1251086. https://doi.org/10.1126/science.1251086.
36. Horneck Johnston, C.J.H., Ledwith, A.E., Lundahl, M.L.E., Charles-Messance, H., Hackett, E.E., O'Shaughnessy, S.D., Clegg, J., Prendeville, H., McGrath, J.P., Walsh, A.M., et al. (2024). Recognition of yeast β-glucan particles triggers immunometabolic signaling required for trained immunity. iScience *27*, 109030. https://doi.org/10.1016/j.isci.2024.109030.
37. Kleinnijenhuis, J., Quintin, J., Preijers, F., Joosten, L.A.B., Ifrim, D.C., Saeed, S., Jacobs, C., van Loenhout, J., de Jong, D., Stunnenberg, H.G., et al. (2012). Bacille Calmette-Guérin induces NOD2-dependent nonspecific protection from reinfection via epigenetic reprogramming of monocytes. Proc. Natl. Acad. Sci. USA *109*, 17537–17542. https://doi.org/10.1073/pnas.1202870109.
38. Levra Levron, C., Watanabe, M., Proserpio, V., Piacenti, G., Lauria, A., Kaltenbach, S., Tamburrini, A., Nohara, T., Anselmi, F., Duval, C., et al. (2023). Tissue memory relies on stem cell priming in distal undamaged areas. Nat. Cell Biol. *25*, 740–753. https://doi.org/10.1038/s41556-023-01120-0.
39. O'Farrell, A., Niu, Z., and Raj, A. (2026). Quantitative Cytokine Profiling of Primary Human Macrophages Reveals Distinct Single-Cell Modes of Trained Immunity. Cell Syst. *17*, 101648. https://doi.org/10.1016/j.cels.2026.101648.
40. Koeken, V.A., de Bree, L.C.J., Mourits, V.P., Moorlag, S.J., Walk, J., Cirovic, B., Arts, R.J., Jaeger, M., Dijkstra, H., Lemmers, H., et al. (2020). BCG vaccination in humans inhibits systemic inflammation in a sex-dependent manner. J. Clin. Invest. *130*, 5591–5602. https://doi.org/10.1172/JCI133935.
41. McLean, C.Y., Bristor, D., Hiller, M., Clarke, S.L., Schaar, B.T., Lowe, C.B., Wenger, A.M., and Bejerano, G. (2010). GREAT improves functional interpretation of cis-regulatory regions. Nat. Biotechnol. *28*, 495–501. https://doi.org/10.1038/nbt.1630.
42. Ferreira, A.V., Domiguéz-Andrés, J., and Netea, M.G. (2022). The Role of Cell Metabolism in Innate Immune Memory. J. Innate Immun. *14*, 42–50. https://doi.org/10.1159/000512280.
43. Cheng, S.-C., Quintin, J., Cramer, R.A., Shepardson, K.M., Saeed, S., Kumar, V., Giamarellos-Bourboulis, E.J., Martens, J.H.A., Rao, N.A., Aghajanirefah, A., et al. (2014). mTOR- and HIF-1α-mediated aerobic glycolysis as metabolic basis for trained immunity. Science *345*, 1250684. https://doi.org/10.1126/science.1250684.
44. Arts, R.J.W., Carvalho, A., La Rocca, C., Palma, C., Rodrigues, F., Silvestre, R., Kleinnijenhuis, J., Lachmandas, E., Gonçalves, L.G., Belinha, A., et al. (2016). Immunometabolic Pathways in BCG-Induced Trained Immunity. Cell Rep. *17*, 2562–2571. https://doi.org/10.1016/j.celrep.2016.11.011.
45. Li, P., Wu, X., Huang, Y., Qin, R., Xiong, P., and Qiu, Y. (2025). L-serine metabolic regulation and host respiratory homeostasis. Front. Cell. Infect. Microbiol. *15*, 1518659. https://doi.org/10.3389/fcimb.2025.1518659.
46. Schep, A.N., Wu, B., Buenrostro, J.D., and Greenleaf, W.J. (2017). chromVAR: inferring transcription-factor-associated accessibility from single-cell epigenomic data. Nat. Methods *14*, 975–978. https://doi.org/10.1038/nmeth.4401.
47. Feng, A.-C., Thomas, B.J., Purbey, P.K., de Melo, F.M., Liu, X., Daly, A.E., Sun, F., Lo, J.H.-H., Cheng, L., Carey, M.F., et al. (2024). The transcription factor NF-κB orchestrates nucleosome remodeling during the primary response to Toll-like receptor 4 signaling. Immunity *57*, 462–477.e9. https://doi.org/10.1016/j.immuni.2024.02.004.
48. Lau, C.M., Adams, N.M., Geary, C.D., Weizman, O.-E., Rapp, M., Pritykin, Y., Leslie, C.S., and Sun, J.C. (2018). Epigenetic control of innate and adaptive immune memory. Nat. Immunol. *19*, 963–972. https://doi.org/10.1038/s41590-018-0176-1.
49. Larsen, S.B., Cowley, C.J., Sajjath, S.M., Barrows, D., Yang, Y., Carroll, T.S., and Fuchs, E. (2021). Establishment, maintenance, and recall of inflammatory memory. Cell Stem Cell *28*, 1758–1774.e8. https://doi.org/10.1016/j.stem.2021.07.001.
50. Li, J., Ravindran, P.T., O'Farrell, A., Busch, G.T., Boe, R.H., Niu, Z., Woo, S., Dunagin, M.C., Jain, N., Goyal, Y., et al. (2026). AP-1 mediates cellular adaptation and memory formation. Nat. Commun. https://doi.org/10.1038/s41467-026-70862-w.
51. Nagaraja, S., Ojeda-Miron, L., Zhang, R., Oreskovic, E., Hock, C., Hu, Y., Zeve, D., Sharma, K., Hyman, R.R., Zhang, Q., et al. (2026). Epigenetic memory of colitis promotes tumour growth. Nature. https://doi.org/10.1038/s41586-026-10258-4.
52. Fanucchi, S., Fok, E.T., Dalla, E., Shibayama, Y., Börner, K., Chang, E.Y., Stoychev, S., Imakaev, M., Grimm, D., Wang, K.C., et al. (2019). Immune genes are primed for robust transcription by proximal long noncoding RNAs located in nuclear compartments. Nat. Genet. *51*, 138–150. https://doi.org/10.1038/s41588-018-0298-2.
53. Bentsen, M., Goymann, P., Schultheis, H., Klee, K., Petrova, A., Wiegandt, R., Fust, A., Preussner, J., Kuenne, C., Braun, T., et al. (2020). ATAC-seq

footprinting unravels kinetics of transcription factor binding during zygotic genome activation. Nat. Commun. *11*, 4267. https://doi.org/10.1038/s41467-020-18035-1.

54. Boutilier, A.J., Raad, M., Paar, K.E., Matissek, S.J., Banks, C.E., Carl, A.L., Murray, J.M., Metzler, A.D., Koeppen, K.U., Gupta, M., et al. (2024). GLI3 is required for M2 macrophage polarization and M2-mediated Waldenström macroglobulinemia growth and survival. Int. J. Mol. Sci. *25*, 13120. https://doi.org/10.3390/ijms252313120.

55. Luan, B., Yoon, Y.-S., Le Lay, J., Kaestner, K.H., Hedrick, S., and Montminy, M. (2015). CREB pathway links PGE2 signaling with macrophage polarization. Proc. Natl. Acad. Sci. USA *112*, 15642–15647. https://doi.org/10.1073/pnas.1519644112.

56. Veremeyko, T., Yung, A.W.Y., Anthony, D.C., Strekalova, T., and Ponomarev, E.D. (2018). Early growth response gene-2 is essential for M1 and M2 macrophage activation and plasticity by modulation of the transcription factor CEBPβ. Front. Immunol. *9*, 2515. https://doi.org/10.3389/fimmu.2018.02515.

57. Gorin, A., Niu, S., Harriott, N., Koduvayur, V., Cheng, Q.J., and Hoffmann, A. (2026). IFNγ-induced memory in human macrophages is sustained by the durability of cytokine signaling itself. J. Exp. Med. *223*. https://doi.org/10.1084/jem.20250976.

58. Kang, K., Bachu, M., Park, S.H., Kang, K., Bae, S., Park-Min, K.-H., and Ivashkiv, L.B. (2019). IFN-γ selectively suppresses a subset of TLR4-activated genes and enhancers to potentiate macrophage activation. Nat. Commun. *10*, 3320. https://doi.org/10.1038/s41467-019-11147-3.

59. Qiao, Y., Giannopoulou, E.G., Chan, C.H., Park, S.-H., Gong, S., Chen, J., Hu, X., Elemento, O., and Ivashkiv, L.B. (2013). Synergistic activation of inflammatory cytokine genes by interferon-γ-induced chromatin remodeling and toll-like receptor signaling. Immunity *39*, 454–469. https://doi.org/10.1016/j.immuni.2013.08.009.

60. Prestwood, T.R., Morar, M.M., Zellweger, R.M., Miller, R., May, M.M., Yauch, L.E., Lada, S.M., and Shresta, S. (2012). Gamma interferon (IFN-γ) receptor restricts systemic dengue virus replication and prevents paralysis in IFN-α/β receptor-deficient mice. J. Virol. *86*, 12561–12570. https://doi.org/10.1128/JVI.06743-11.

61. Mikloska, Z., and Cunningham, A.L. (2001). Alpha and gamma interferons inhibit herpes simplex virus type 1 infection and spread in epidermal cells after axonal transmission. J. Virol. *75*, 11821–11826. https://doi.org/10.1128/JVI.75.23.11821-11826.2001.

62. Changotra, H., Jia, Y., Moore, T.N., Liu, G., Kahan, S.M., Sosnovtsev, S.V., and Karst, S.M. (2009). Type I and type II interferons inhibit the translation of murine norovirus proteins. J. Virol. *83*, 5683–5692. https://doi.org/10.1128/JVI.00231-09.

63. Drayman, N., Patel, P., Vistain, L., and Tay, S. (2019). HSV-1 single-cell analysis reveals the activation of anti-viral and developmental programs in distinct sub-populations. eLife *8*, e46339. https://doi.org/10.7554/eLife.46339.

64. Gottschalk, R.A. (2023). Signaling is the pathway to macrophage function. Trends Immunol. *44*, 496–498. https://doi.org/10.1016/j.it.2023.04.007.

65. Luecke, S., Sheu, K.M., and Hoffmann, A. (2021). Stimulus-specific responses in innate immunity: Multilayered regulatory circuits. Immunity *54*, 1915–1932. https://doi.org/10.1016/j.immuni.2021.08.018.

66. Lavin, Y., Winter, D., Blecher-Gonen, R., David, E., Keren-Shaul, H., Merad, M., Jung, S., and Amit, I. (2014). Tissue-resident macrophage enhancer landscapes are shaped by the local microenvironment. Cell *159*, 1312–1326. https://doi.org/10.1016/j.cell.2014.11.018.

67. Liu, S.X., Gustafson, H.H., Jackson, D.L., Pun, S.H., and Trapnell, C. (2020). Trajectory analysis quantifies transcriptional plasticity during macrophage polarization. Sci. Rep. *10*, 12273. https://doi.org/10.1038/s41598-020-68766-w.

68. Niu, Z., Bruyère, T., Manthey, D., Li, J., O'Farrell, A., and Raj, A. (2025). NimbusImage: a cloud-computing platform for image analysis. Nat. Methods *23*, 6–8.

69. Niu, Z., O'Farrell, A., Li, J., Reffsin, S., Jain, N., Dardani, I., Goyal, Y., and Raj, A. (2025). Piscis: A loss estimator of the F1 score enables accurate spot detection in fluorescence microscopy images via deep learning. Cell Syst. *16*, 101448. https://doi.org/10.1016/j.cels.2025.101448.

70. Wei, Z., Zhang, W., Fang, H., Li, Y., and Wang, X. (2018). esATAC: an easy-to-use systematic pipeline for ATAC-seq data analysis. Bioinformatics *34*, 2664–2665. https://doi.org/10.1093/bioinformatics/bty141.

71. Ou, J., Liu, H., Yu, J., Kelliher, M.A., Castilla, L.H., Lawson, N.D., and Zhu, L.J. (2018). ATACseqQC: a Bioconductor package for post-alignment quality assessment of ATAC-seq data. BMC Genomics *19*, 169. https://doi.org/10.1186/s12864-018-4559-3.

72. Zhang, Y., Liu, T., Meyer, C.A., Eeckhoute, J., Johnson, D.S., Bernstein, B.E., Nusbaum, C., Myers, R.M., Brown, M., Li, W., et al. (2008). Model-based analysis of ChIP-Seq (MACS). Genome Biol. *9*, R137. https://doi.org/10.1186/gb-2008-9-9-r137.

73. Lawrence, M., Huber, W., Pagès, H., Aboyoun, P., Carlson, M., Gentleman, R., Morgan, M.T., and Carey, V.J. (2013). Software for computing and annotating genomic ranges. PLoS Comput. Biol. *9*, e1003118. https://doi.org/10.1371/journal.pcbi.1003118.

74. Love, M.I., Huber, W., and Anders, S. (2014). Moderated estimation of fold change and dispersion for RNA-seq data with DESeq2. Genome Biol. *15*, 550. https://doi.org/10.1186/s13059-014-0550-8.

75. Fornes, O., Castro-Mondragon, J.A., Khan, A., van der Lee, R., Zhang, X., Richmond, P.A., Modi, B.P., Correard, S., Gheorghe, M., Baranašić, D., et al. (2020). JASPAR 2020: update of the open-access database of transcription factor binding profiles. Nucleic Acids Res. *48*, D87–D92. https://doi.org/10.1093/nar/gkz1001.

76. Raj, A., van den Bogaard, P., Rifkin, S.A., van Oudenaarden, A., and Tyagi, S. (2008). Imaging individual mRNA molecules using multiple singly labeled probes. Nat. Methods *5*, 877–879. https://doi.org/10.1038/nmeth.1253.

77. Corces, M.R., Corces, M.R., Trevino, A.E., Hamilton, E.G., Greenside, P.G., Sinnott-Armstrong, N.A., Vesuna, S., Satpathy, A.T., Rubin, A.J., Montine, K.S., et al. (2017). Omni-ATAC-seq: Improved ATAC-seq protocol. Protocol exchange. protocols.io. https://doi.org/10.1038/protex.2017.096.

Please cite this article in press as: O'Farrell et al., Human macrophages encode stimulus-specific information of prior exposures through trained immunity, Cell Systems (2026), https://doi.org/10.1016/j.cels.2026.101647

STAR★METHODS

KEY RESOURCES TABLE

REAGENT or RESOURCE	SOURCE	IDENTIFIER
Antibodies		
anti-CD80	BioLegend	Cat: 305217; RRID: AB_1877254
anti-CD206	BioLegend	Cat: 321151; RRID: AB_2860838
anti-CD284 (TLR4)	BioLegend	Cat: 312805; RRID: AB_314954
anti-CD369 (Dectin-1)	BioLegend	Cat: 355403; RRID: AB_2562060
Zombie Green	BioLegend	Cat: 423111
7AAD Live/Dead Stain	BioLegend	Cat: 420403
Fc Block	BD	Cat: 564219
pSTAT1 Rabbit anti-Human mAb	Cell Signaling	Cat: 9167T; RRID: AB_561284
pp65 Rabbit anti-Human Antibody	Cell Signaling	Cat: 3033T; RRID: AB_331284
Anti-Rabbit Secondary F(ab)2, A594	Cell Signaling	Cat: 8889S; RRID: AB_2716249
Bacterial and virus strains		
HSV-1 (ICP4-YFP)	Dr. Nir Drayman, UC Irvine	N/A
Biological samples		
Human monocytes from apheresis product of healthy donors	University of Pennsylvania Human Immunology Core	See Table S1
Chemicals, peptides, and recombinant proteins		
β-D-Glucan	Thomas Scientific	C940X31
Muramyl Dipeptide (MDP)	Invivogen	tlrl-mdp
Interferon Gamma	Gibco	PHC4031
Oxidized low-density lipoprotein (oxLDL)	Invitrogen	L34357
CpG ODN 2395	Invivogen	tlrl-2395
Poly I:C	Invitrogen	tlrl-pic
TGF-β	Sigma-Aldrich	T7039
Lipopolysaccharide (LPS)	Invitrogen	501122025
Zymosan	Invivogen	tlrl-zyn
Tn5	Dr. Kavitha Sarma, Wistar Institute	N/A
pH-rodo Red E Coli BioParticles Conjugate	Invitrogen	P35361
Deposited data		
Raw ATACseq data	This paper	GEO: GSE323311
ENCODE blacklist regions	Encyclopedia of DNA Elements (ENCODE)	https://github.com/Boyle-Lab/Blacklist/blob/master/lists/hg38-blacklist.v2.bed.gz
Oligonucleotides		
Oligonucleotides for single-molecule RNA FISH	IDT	See Table S2
ATACseq Primers	IDT	See Table S3
Software and algorithms		
RNA FISH Probe Design	Laboratory of Arjun Raj	https://github.com/arjunrajlaboratory/ProbeDesign
NimbusImage	Laboratory of Arjun Raj; Niu et al.[68]	https://github.com/arjunrajlaboratory/NimbusImage
Piscis	Laboratory of Arjun Raj; Niu et al.[69]	https://github.com/zjniu/Piscis
Code for analysis and figure generation	This paper	https://doi.org/10.5061/dryad.stqjq2cjc
Rbowtie2	Wei et al.[70]	https://bioconductor.org/packages/Rbowtie2/

(*Continued on next page*)

Continued

REAGENT or RESOURCE	SOURCE	IDENTIFIER
ATACseqQC	Ou et al.[71]	https://bioconductor.org/packages/ATACseqQC/
Picard	The Broad Institute	https://broadinstitute.github.io/picard/
MACS2	Zhang et al.[72]	https://pypi.org/project/MACS2/
GenomicAlignments	Lawrence et al.[73]	https://bioconductor.org/packages/GenomicAlignments/
DESeq2	Love et al.[74]	https://bioconductor.org/packages/DESeq2/
GREAT	McLean et al.[41]	http://great.stanford.edu
JASPAR2020	Fornes et al.[75]	https://bioconductor.org/packages/JASPAR2020/
chromVAR	Schep et al.[46]	https://bioconductor.org/packages/chromVAR/
TOBIAS	Bentsen et al.[53]	https://github.com/loosolab/TOBIAS

EXPERIMENTAL MODEL AND STUDY PARTICIPANT DETAILS

Deidentified human immune cells were collected from the apheresis product of healthy donors at the Perelman School of Medicine at the University of Pennsylvania by the Human Immunology Core. Deidentified donor information (age, sex, and date of sample collection) can be found in Table S1. Monocytes were isolated by negative selection with StemCell RosetteSep kits. Isolated monocytes were cultured in RPMI supplemented with 25mM HEPES, 1% penicillin/streptomycin, and 10% fetal bovine serum, and initially seeded at a density of 800,000 cells per milliliter in Cellvis 24 well glass imaging plates (Fisher NC0397150) or Cellvis 96 well glass imaging plates (Fisher P96-1.5H-N).

METHOD DETAILS

Induction of Trained Immunity

We followed an *in vitro* procedure of training commonly used in literature.[22] We introduced training ligands at the following concentrations: β-Glucan at 5 μg/mL, MDP at 1 μg/mL, IFNγ at 50 ng/mL, CpG at 100 ng/mL, Poly I:C at 10 μg/mL, TGF-β at 2 ng/mL, and oxLDL at 10 μg/mL. We chose these doses based on thorough comparison to published literature. To generate trained cells, we stimulated with training ligand during the first 24 hours of culture, while untrained cells received no stimulation. After 24 hours, we removed the training ligand by washing all wells (including untrained controls) twice with PBS, then allowed the cells to rest for five additional days, during which time the cells differentiated into monocyte-derived macrophages. On the sixth day of culture, we evaluated trained cells before secondary stimulation, or after stimulation with a readout stimulus. Unless otherwise stated, stimulation on day 6 with lipopolysaccharide (LPS) was at a dose of 100 ng/mL, and stimulation with zymosan was at a dose of 10 μg/mL. For durability studies, cells were restimulated with 100 ng/mL LPS on day 11.

Single-Molecule RNA Fluorescence In-Situ Hybridization (RNA FISH)

Oligonucleotides complementary to the transcripts for *TNF*, *CXCL10*, and *IL6* were designed using custom Matlab software (https://github.com/arjunrajlaboratory/ProbeDesign) and purchased from IDT. Due to the short length of these transcripts, we included the 3' UTR in each target sequence, to generate a total of 24 oligonucleotide probes per gene. Full sequences for each of these probes can be found in Table S2. To generate fluorescent probes, we first added an amine group to the 3′ end of each oligonucleotide using terminal transferase (TDT), then coupled to either CY3, Alexa 594, or Atto 700 dye.

Single-molecule RNA FISH was performed as described previously.[76] Briefly, cells were fixed in 4% paraformaldehyde for 10 minutes, then permeabilized using 70% ethanol overnight at 4°C. Immediately before probe addition, cells were briefly washed in 5% sodium dodecyl sulfate (SDS) for 1 minute to reduce autofluorescence.

To perform *in situ* hybridization, we diluted probes in hybridization buffer (10% formamide and 10% dextran sulfate in 2X saline sodium citrate (SSC) buffer) before incubating overnight at 37°C covered with a glass coverslip. Cells were then stained with DAPI for 30 minutes, then imaged in 2X saline sodium citrate (SSC) buffer. Samples were imaged across 5 Z-planes on an inverted Nikon TI-E microscope at 60X magnification.

RNA FISH images were analyzed in the custom imaging software NimbusImage.[68] NimbusImage is an open-source, in-browser program that allows for direct visualization and analysis of large imaging datasets, and includes in-built analysis tools such as Cellpose, Segment-Anything, and Piscis.

Images were uploaded to NimbusImage, and cell cytoplasm was manually segmented using the ''Manual Blob Annotation'' tool. RNA FISH spots were identified in all Z planes using the deep learning algorithm Piscis.[69] Piscis is a deep neural network

Please cite this article in press as: O'Farrell et al., Human macrophages encode stimulus-specific information of prior exposures through trained immunity, Cell Systems (2026), https://doi.org/10.1016/j.cels.2026.101647

classification algorithm that employs a novel loss function (the SmoothF1 loss) to account for class imbalance inherent to RNA FISH spot detection during training, ensuring accurate spot detection. Following identification, spots were counted and assigned to each cell using the "Point Count 3D Projection" tool in NimbusImage. Proportions of cells expressing each gene were calculated using a threshold of 1 spot per cell after manual noise correction.

Functional Analysis of Phagocytosis and Viral Infection

To evaluate phagocytosis efficacy, trained and untrained cells were stimulated with 100μg/mL of pH-rodo labeled E Coli BioParticles (Invitrogen) for 30 minutes or 1 hour. After stimulation, cells were fixed and DAPI stained, and imaged on an inverted Nikon TI-E microscope at 40X magnification, with fluorescence measured in the Alexa 594 channel. Images were uploaded to NimbusImage, cell cytoplasm was manually segmented, and mean fluorescence per cell was calculated using the "Blob Mean Intensity" tool in NimbusImage.

For viral infection, we used an HSV-1 virus with a YFP fluorescent tag on the ICP4 locus (kind gift of Dr. Nir Drayman, UC Irvine).[63] Cells were first washed with PBS before infection at a MOI of 2. After 1 hour, the virus was removed and cells remained in culture for 5 additional hours, after which time they were fixed and DAPI stained. Cells were imaged on an inverted Nikon TI-E microscope at 40X magnification, with fluorescence measured in the YFP channel. Images were uploaded to NimbusImage, nuclei segmented using a combination of Cellpose and SegmentAnything in NimbusImage, and fluorescence per nucleus was calculated using the "Blob Mean Intensity" tool in NimbusImage. Infected cells were identified by mean nuclear YFP fluorescence five standard deviations higher than the mean YFP fluorescence measured in uninfected cells.

Flow Cytometry

Cells were harvested for flow cytometry by first incubating in PBS + 10mM EDTA for 10 minutes on ice, then detaching by vigorous pipetting. Cells were resuspended in Fc block (1:100) for 10 minutes at room temperature and protected from light. Antibodies were diluted to a concentration of 1:100 in FACS buffer and incubated with samples for 30 minutes at 4°C, protected from light. Cell viability was assessed using Zombie Green Live/Dead stain (1:1000) for CD80/CD206 analysis, and using 7AAD Live/Dead stain (1:100) for Dectin1/TLR4 analysis. Samples were collected on a BD LSR II flow cytometer, and analyzed using FlowJo version 10.8.1.

Immunofluorescence

Trained and untrained cells were assessed before, or 5, 10, or 20 minutes after restimulation. When assessing pp65, cells were restimulated with 100 ng/mL LPS. When assessing pSTAT1, cells were restimulated with 50 ng/mL IFNγ.

Cells were fixed in 4% formaldehyde, permeabilized with 0.2% Triton-X, and blocked with 5% bovine serum albumin (BSA). Cells were incubated with primary antibody (phospho-p65 at 1:1600 in PBS + 1.5% BSA, phospho-STAT1 at 1:800 in PBS + 1.5% BSA) overnight at 4°C. Cells were then incubated with secondary antibody (1:1500) and DAPI for one hour at room temperature, then imaged on an inverted Nikon TI-E microscope at 40X magnification, with fluorescence measured in the Alexa 594 channel. Images were uploaded to NimbusImage, nuclei segmented using a combination of Cellpose and SegmentAnything in NimbusImage, and fluorescence per nucleus was calculated using the "Blob Mean Intensity" tool in NimbusImage.

ATAC Sequencing

We performed a modified form of the OMNI-ATAC sequencing protocol described in Corces et al.,[77] on untrained, βG-trained, MDP-trained, and IFNγ-trained cells from three donors. In a separate sequencing run, we sequenced untrained, βG-trained, MDP-trained, IFNγ-trained, CpG-trained, oxLDL-trained, and PolyIC-trained cells from one donor. For Donor ND410b, we collected untrained, βG-trained, MDP-trained, and IFNγ-trained cells on both day 6 and day 11 of culture.

We collected 100,000 cells per technical duplicate, and lysed cells in buffer containing 10% NP-40, 10% Tween-20, and 1% Digitonin for 3 minutes at 4°C. Lysed cells were transposed with Tn5 (kind gift of Dr. Kavitha Sarma, Wistar Institute) for 30 minutes at 37°C. Transposed genomic DNA was isolated using a Zymo DNA Clean and Concentrator kit, then amplified using custom primers described in Table S3 (originally designed by Greenleaf Lab, Stanford University) for 13 PCR cycles. Libraries were purified using double-sided selection with AMPure XP magnetic beads, and final concentration measured by BioAnalyzer High Sensitivity DNA chips. Libraries were sequenced at depth of approximately 50 million paired-end reads per sample on a NextSeq2000 with a P4 XLEAP 100-cycle kit.

To ensure the highest possible sample quality, we transposed live cells from each donor as they became available. A control sample of MDA-MB-231 cancer cells processed alongside two of these batches showed nearly identical accessibility profiles (Figure S5C), demonstrating that batch-to-batch variability was minimal, and did not drive observed variability across individual donors.

Sequencing reads were first aligned to hg38 using bowtie2. Bam files were cleaned and Tn5 shift was performed using the *bamQC* and *shiftGAlignmentsList* functions from the Bioconductor package ATACseqQC.[71] PCR duplicates were removed using Picard's *MarkDuplicates* function.

To call peaks, we used the *callpeak* function from MACS2,[72] with an FDR cutoff of 0.05, inputting replicate-merged samples filtered to a fragment size less than 300 base pairs to improve accuracy. Once peak regions were identified, we generated one nonredundant peak list shared across all samples and donors, filtered to only include peaks present in at least two samples, and not listed in the

Please cite this article in press as: O'Farrell et al., Human macrophages encode stimulus-specific information of prior exposures through trained immunity, Cell Systems (2026), https://doi.org/10.1016/j.cels.2026.101647

ENCODE blacklist regions. We then used GenomicAlignment's[73] *summarizeOverlaps* function to generate a full counts matrix for all samples (keeping technical replicates separate, and not filtered by fragment size).

To identify differential regions of chromatin, we set a minimum threshold of 20 reads per peak, before normalizing by read depth and averaging the read counts of technical replicates for each peak. We then used DESeq2[74] to identify differentially accessible regions between each trained condition and our untrained samples, for each donor. We selected regions deemed statistically significantly differentially accessible (padj < 0.05) from untrained cells in at least two of our three donors. For these "highly confident regions," we performed gene enrichment analysis compared against the full peak list using *GREAT*,[41] which connects regions of interest to their closest nearby gene, then identifies enriched gene ontologies compared against the entire nonredundant peak list. We set a cutoff of FDR < 0.05 for significantly enriched *GO* terms.

We used the Bioconductor packages JASPAR2020[75] and chromVAR[46] to identify differential transcription factor motif enrichment across samples. The *computeDeviations* function was run on the counts matrix for each donor separately, with *getBackgroundPeaks* and *computeExpectations* set to the untrained samples from that donor to compare trained counts against an appropriate background. The function *deviationScores* was used to calculate z score enrichment for each identified motif.

To identify differentially bound factors within our identified peaks, we used TOBIAS[53] functions *ATACorrect* to identify regions of Tn5 protection (suggestive of actively bound factors) and *ScoreBigwig* to calculate footprinting scores. Differentially enriched motifs at these footprints were identified using *BINDetect*, with highlighted differential factors above the 95% quantile of -log10(p-value) and/or above the 95% quantile and below the 5% quantile of differential binding scores. We then filtered this list to those factors highlighted at least two of our three donors.

QUANTIFICATION AND STATISTICAL ANALYSIS

To calculate statistical significance across proportions of *IL6* and *CXCL10* responders in trained and untrained cells, we used the following equation: $z = \frac{(p_{trained} - p_{untrained})}{\sqrt{p_{total}(1-p_{total})\left(\frac{1}{n_{trained}} + \frac{1}{n_{untrained}}\right)}}$, where $p_{trained}$ is the proportion of responders in the trained population, $p_{untrained}$ is the proportion of responders in the untrained population, p_{total} is the overall sample proportion, and $n_{trained}$ and $n_{untrained}$ are the sample sizes. We then used the *pnorm()* function in R to convert the z-score to a p-value, using a two-tailed test for statistical significance.

To calculate statistical significance for difference in proportion of cells infected with HSV-1, we used the following equation: $z = \frac{(p_{trained} - p_{untrained})}{\sqrt{p_{total}(1-p_{total})\left(\frac{1}{n_{trained}} + \frac{1}{n_{untrained}}\right)}}$, where $p_{trained}$ is the proportion of infected cells in the trained population, $p_{untrained}$ is the proportion of infected in the untrained population, p_{total} is the overall sample proportion of infected cells, and $n_{trained}$ and $n_{untrained}$ are the sample sizes. We then used the *pnorm()* function in R to convert the z-score to a p-value, using a two-tailed test for statistical significance.

To calculate statistical significance for differences in mean nuclear intensity of immunofluorescence signal, we used the *t.test()* function in R to calculate the p-value for a two-tailed test for statistical significance, then calculated the log2 fold change of mean nuclear intensity across conditions.